1   ***Artemisia* pollen dataset for exploring the potential ecological**

2   **indicators in deep time**

3   Li-Li Lu[a,d†], Bo-Han Jiao [a,d†], Feng Qin [b†], Gan Xie[a†], Kai-Qing Lu[a,d], Jin-Feng Li[a], Bin Sun[a], Min Li[a],

4   David K. Ferguson[c], Tian-Gang Gao[a,d *], Yi-Feng Yao[a,d*], Yu-Fei Wang[a,d*]

5   *[a]State Key Laboratory of Systematic and Evolutionary Botany, Institute of Botany, Chinese Academy of*

6   *Sciences, 20 Nanxincun Xiangshan, Beijing 100093, China*

7   *[b]Key Laboratory of Land Surface Pattern and Simulation, Institute of Geographic Sciences and Natural*

8   *Resources Research, Chinese Academy of Sciences, Beijing 100101, China*

9   *[c]University of Vienna, Institute of Palaeontology, Althanstrasse 14, Vienna A-1090, Austria*

10   *[d]University of Chinese Academy of Sciences, Beijing 100049, China*

11   [†] These authors contributed equally to this work.

12   [*]Corresponding authors. Tel: +86 (10) 62836439.

13   Email addresses: gaotg@ibcas.ac.cn (T. G. GAO); yaoyf@ibcas.ac.cn (Y. F. YAO); wangyf@ibcas.ac.cn (Y.

14   F. WANG).

15 **Abstract.** *Artemisia*, along with Chenopodiaceae is the dominant component growing in the desert and dry

16 grassland of the Northern Hemisphere. *Artemisia* pollen with its high productivity, wide distribution, and easy

17 identification, is usually regarded as an eco-indicator for assessing aridity and distinguishing grassland from

18 desert vegetation in terms of the pollen relative abundance ratio of Chenopodiaceae/*Artemisia* (C/A).

19 Nevertheless, divergent opinions on the degree of aridity evaluated by *Artemisia* pollen have been circulating

20 in the palynological community for a long time. To solve the conclusion, we first selected 36 species from 9

21 clades and 3 outgroups of *Artemisia* based on the phylogenetic framework, which attempts to cover the

22 maximum range of pollen morphological variation. Then, sampling, experiments, photography, and

23 measurements were taken using standard methods. Here, we present pollen datasets containing 4018 original

24 pollen photographs, 7200 statistical pollen morphological traits, information on 30858 source plant

25 occurrences, and corresponding environmental factors. Hierarchical cluster analysis on pollen morphological

26 traits was carried out to subdivide *Artemisia* pollen into three types. When plotting the three pollen types of

27 *Artemisia* onto the global terrestrial ecoregions, different pollen types of *Artemisia* were found to have

28 different habitat ranges. These findings change the traditional concept of *Artemisia* being restricted to arid and

29 semi-arid environments. The data framework that we designed is open and expandable for new pollen data of

30 *Artemisia* worldwide. In the future, linking pollen morphology with habitat via these pollen datasets will

31 create additional knowledge that will increase the resolution of the ecological environment in the geological

32 past. The *Artemisia* pollen datasets are freely available at Zenodo (https://doi.org/10.5281/zenodo.5842909;

33 Lu and Jiao, 2022).

1 Introduction

The concept of global change could be regarded as any consistent trend in the environment - past, present, or projected - that affects a substantial part of the globe, following the definition given in the journal Global Change Biology. Especially importantly, past climates shed light on our future (Tierney et al., 2020). When attempting to reconstruct past global change prior to meteorological records, we need some appropriate biological or abiotic proxies based on long-term, consistently collected data, e.g. leaf wax biomarkers (Bhattacharya et al., 2018), tree-ring data (Moberg et al., 2005), leaf form (Yang et al., 2015), pollen data (Mosbrugger et al., 2005; Guiot and Cramer, 2016; Marsicek et al., 2018), atmospheric carbon dioxide (Zachos et al., 2008; Beerling and Royer, 2011), and isotope records (Zachos et al., 2001; Sánchez-Murillo et al., 2019). Determining a suitable proxy to reconstruct palaeoclimate and palaeoenvironment is a great scientific challenge (Tierney et al., 2020; Mcclelland et al., 2021).

The pollen of *Artemisia* (A), together with that of Chenopodiaceae (C) in arid and semi-arid areas, in the form of the ratio of C/A pollen abundance, was applied to distinguish grassland and desert vegetation types and assess the degree of drought in the geological past (El-Moslimany, 1990; Sun et al., 1994; Davies and Fall, 2001; Herzschuh et al., 2004; Xu et al., 2007; Zhao et al., 2009; Zhang et al., 2010; Zhao et al., 2012; Li et al., 2017; Ma et al., 2017; Koutsodendris et al., 2019; Wang et al., 2020), because both Chenopodiaceae and *Artemisia* are dominant elements of desert vegetation (China Vegetation Editorial Committee, 1980; Vrba, 1980; Tarasov et al., 1998; Herzschuh et al., 2004; Li et al., 2010; Zhao et al., 2021), and the sum of their pollen relative abundances in the surface soil is usually more than 50% in arid and semi-arid areas (Sun et al., 1994; Lu et al., 2020).

Among them, the pollen of *Artemisia*, with its high productivity, wide spatial and temporal distribution, easy identification, and morphological uniformity under the light microscope (LM), is an essential component and useful bio-indicator in pollen-based past vegetation reconstructions and environmental assessments. Some researchers regarded *Artemisia* as an arid indicator (El-Moslimany, 1990; Yi et al., 2003b; Yi et al., 2003a; Liu et al., 2006; Cai et al., 2019; Cui et al., 2019; Chen et al., 2020; Wu et al., 2020; Cao et al., 2021), while others suggested that the correlation between the relative abundance of *Artemisia* pollen and humidity was insignificant (Weng et al., 1993; Sun et al., 1996; Koutsodendris et al., 2019; Lu et al., 2020; Zhao et al., 2021). Therefore, we need to evaluate the habitat heterogeneity of *Artemisia* with different pollen types when possible.

63   In the past, *Artemisia* pollen was regarded as very uniform under LM (Wodehouse, 1926; Sing and Joshi,

64   1969; Ling, 1982; Wang et al., 1995). For instance, following the description and statistics of pollen

65   morphology of 27 species of *Artemisia* in Eurasia under LM, Sing and Joshi (1969) stated that the pollen

66   grains of *Artemisia* are consistent and continuous in morphology. Later, some authors recognized a series of

67   pollen types (Chen, 1987; Jiang et al., 2005; Ghahraman et al., 2007; Shan et al., 2007; Hayat et al., 2009;

68   Hayat et al., 2010; Hussain et al., 2019), based on a detailed survey of the pollen micromorphology of

69   different taxa under the scanning electron microscope (SEM).

70   For example, Chen (1987) described the pollen morphology of 77 *Artemisia* species from China under

71   LM and SEM and divided these pollen grains into six types by using pollen characters, such as the shape and

72   size of the spinules as well as the density of spinules and granules. Type I (sparse spinules with granules

73   among them), type II (dense spinules, no or few granules), type III (sparse spinules, no granules), type IV

74   (dense spinules, well-developed granules), type V (small and sparse spinules, smooth tectum) and type VI

75   (dissimilar spinules with granules among them).

76   Shan et al. (2007) investigated the pollen morphology of 32 *Artemisia* species from the Loess Plateau of

77   China under LM and SEM and divided these pollen grains into five types according to exine sculpture: type I

78   (dense spinules with swollen bases, small granules), type II (dense spinules, swollen bases almost united),

79   type III (dense spinules with swollen bases and smooth tectum), type IV (sparse small spinules and smooth

80   tectum) and type V (sparse spinules, small granules).

81   Jiang et al. (2005) observed the pollen morphology of 57 representative plants in 7 groups of *Artemisia*

82   under LM and SEM. This pollen can be divided into two types based on exine sculpture: type I (spinules

83   multi-ruminated with flared bases, connecting the mostly densely arranged spinules) and type II (densely or

84   loosely arranged spinules without flared bases, interspace glandular or smooth) with subtypes II-1, II-2, II-3,

85   and II-4 based on the distribution of the spinules.

86   Ghahraman et al. (2007) studied the pollen morphology of 26 species of the 33 *Artemisia* species in Iran

87   under LM and SEM. Based on exine ornamentation observed under SEM, two types of pollen grains were

88   recognized: type I, exine surface covered with dense acute spinules, Type II, exine surface with few spinules.

89   Hayat et al. (2009, 2010) carried out a palynological study of 22 *Artemisia* species from Pakistan under

90   LM and SEM. Earlier work demonstrated the phylogenetic associations within *Artemisia* based on a

91   phylogenetic analysis of 9 characters (pollen type, pollen shape, spinule arrangement, exine sculpture, spinule

92   base, the length of polar axis, the length of equatorial axis, exine thickness, and colpus width) of pollen grains

93   of *Artemisia*. In the latter work, eight micromorphological characters were identified and pooled by cluster

94   analysis, leading to the recognition of 5 groups.

95   Hussain et al. (2019) studied the pollen morphology of 15 *Artemisia* species in the Gilgit-Baltistan region

96   of Pakistan utilizing SEM and divided these species into four groups based on cluster analysis of seven

97   micromorphological characters (pollen type, pollen shape, spinule arrangement, exine sculpture, spinule base,

98   polar length, and equatorial width).

99   Almost all of the above-mentioned *Artemisia* pollen classifications were designed to solve taxonomic or

100   phylogenetic problems, and only a few were concerned with linking diverse habitats to the different pollen

101   types in *Artemisia*.

102   Here we attempt to 1) present abundant pollen photographs of 36 species from 9 branches and 3

103   outgroups of the genus (ca. 400 species worldwide, see Ling, 1982; Bremer and Humphries, 1993),

104   constrained by the phylogenetic framework of *Artemisia* (Sanz et al., 2008; Malik et al., 2017); 2) describe

105   and measure the morphological traits of these pollen grains; 3) provide a new classification of pollen types

106   and their distribution worldwide, with a key to pollen types in *Artemisia*; 4) explore the diverse ecological

107   niches of *Artemisia* represented by different pollen types in order to evaluate palaeovegetation and reconstruct

108   palaeoenvironments.

109   **2 Materials and methods**

110   **2.1 Sampling strategy**

111   The 36 pollen samples studied were selected from voucher sheets in the PE herbarium at the Institute of

112   Botany, Chinese Academy of Sciences (Fig. 1, Table B1), covering 9 main clades, i.e., Subg. *Tridentata*, Subg.

113   *Artemisia* (contains Sect. *Artemisia*, Sect. *Abrotanum* I, Sect. *Abrotanum* II and Sect. *Abrotanum* III), Subg.

114   *Pacifica*, Subg. *Seriphidium*, Subg. *Absinthium*, and Subg. *Dracunculus*, constrained by the phylogenetic

115   framework of *Artemisia* (Malik et al., 2017) and 3 outer groups (Sanz et al., 2008), reflecting the maximum

116   diversity or morphological variation under LM and SEM.

117

Figure 1. Phylogenetic tree of *Artemisia* (modified from Malik et al., 2017). The styles of the strokes that
were used to draw the branches indicate the traditional subgeneric classification of *Artemisia*, and the yellow
spots indicate sampled taxa.

2.2 Pollen processing

Pollen samples were acetolyzed by the standard method (Erdtman, 1960) and fixed in glycerine jelly. Standard

procedures were followed for LM and SEM. The pollen grains were photographed under LM (Leica DM 4000)

at a magnification of ×1000 and SEM (Hitachi S-4800) at an accelerating voltage of 30 kV. The pollen

terminology followed the descriptions of Hesse et al. (2009) and Halbritter et al. (2018). The statistical pollen

126 morphological traits of each species were measured from 20 pollen grains under LM and 5 pollen grains under

127 SEM including pollen grain size, colporate pattern, and exine ornamentation. The mean value (M) and

128 standard deviation (SD) of the pollen grains of each species were measured and calculated in both polar and

129 equatorial views (Appendix A, Table 1).

130   The specimen sampling coordinates of the corresponding taxa were obtained from the Global

131 Biodiversity Information Facility (GBIF, https://www.gbif.org/). The corresponding environmental factors

132 including altitude and 19 climate parameters of these coordinates were obtained from WorldClim

133 (https://www.worldclim.org/) with a spatial resolution of 30 seconds (~1 km^2) in 1970-2000.

2.3 Data processing

135 OriginPro 2021 software was used for hierarchical cluster analysis on *Artemisia* pollen data. The Euclidean

136 distance was calculated after the normalization of the original data, and the Ward method was used for

137 clustering. Five groups were established, and the center point of each group was calculated according to the

138 sum of distances. OriginPro 2021 software was used to draw group violin diagrams and run an ANOVA to test

139 for an overall difference between the pollen characters of 3 pollen types, followed by post hoc tests (Tukey).

140 OriginPro 2021 software was also used to run correlation coefficients analysed by the Pearson correlation

141 between pollen morphological traits and environmental factors as well as draw group violin diagrams and run

142 a KWANOVA to test for overall differences between the environmental factors of the 3 pollen types. The

143 images of habitats reproduced in the text are from the websites listed in Table B1.

144   The global distribution data of the 36 representative species and 3 pollen types were plotted on the map

145 of terrestrial ecological regions (Olson et al., 2001) using ArcGIS 10.2 software (Figs. 15, 18). Modern

146 altitude and climatic parameters of corresponding coordinates were obtained by Extract MultiValues To Points

147 using ArcGIS 10.2 software in bilinear interpolation.

3 Data description

3.1 *Artemisia* pollen grains and their source plant habitats

150 Here we provide detailed data on pollen morphological traits, covering 36 species from 9 main clades of

151 *Artemisia* and 3 outgroups constrained by the phylogenetic framework (Sanz et al., 2008; Malik et al., 2017)

152 under LM and SEM, the habitats of their source plants (Figs. 1-13).

153
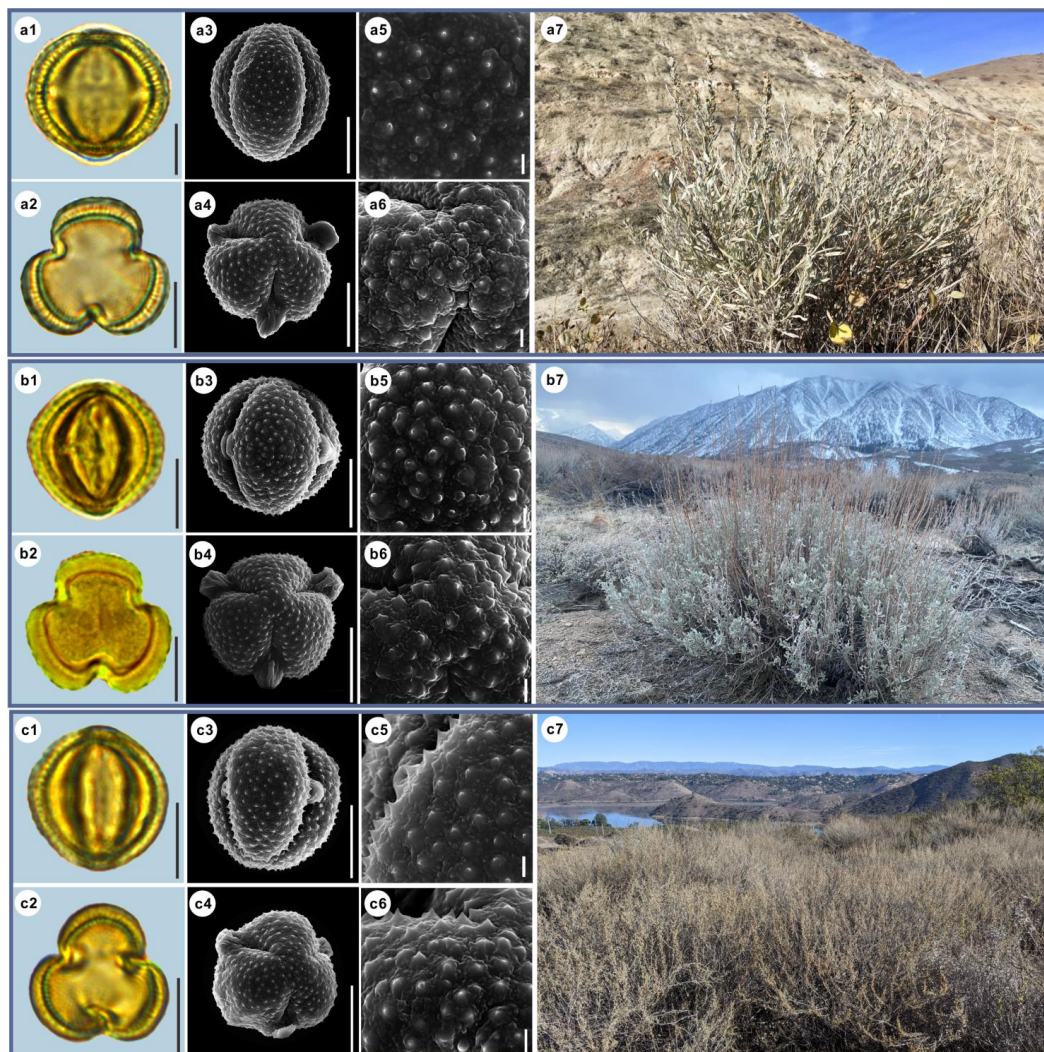
Figure 2. Pollen grains and the habitats of their source plants.

a. *Artemisia cana*; b. *Artemisia tridentata*; c. *Artemisia californica*.

Pollen grains in equatorial view under LM (a1, b1, c1) and SEM (a3, a5, b3, b5, c3, c5), in polar view under

LM (a2, b2, c2) and SEM (a4, a6, b4, b6, c4, c6), along with the habitats of their source plants (a7 cited from

https://www.inaturalist.org/photos/54492753 by © Jason Headley, b7 cited from

https://www.inaturalist.org/photos/117436654 by © Matt Berger, c7 cited from

https://www.inaturalist.org/photos/108921528 by © Don Rideout).

Scale bar in LM and SEM overview 10 μm, in SEM close-up 1 μm.
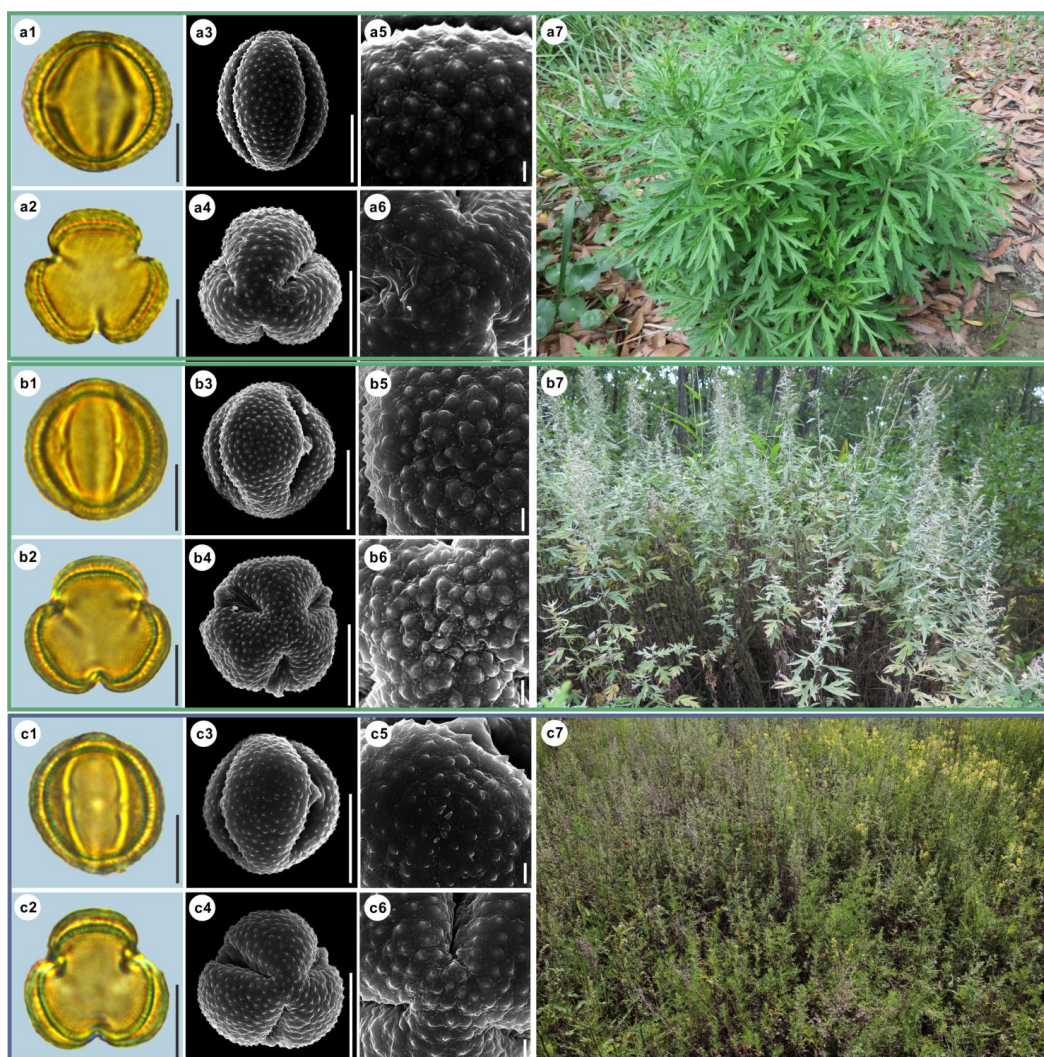
Figure 3. Pollen grains and the habitats of their source plants.

a. *Artemisia indica*; b. *Artemisia argyi*; c. *Artemisia mongolica*.

Pollen grains in equatorial view under LM (a1, b1, c1) and SEM (a3, a5, b3, b5, c3, c5), in polar view under LM (a2, b2, c2) and SEM (a4, a6, b4, b6, c4, c6), along with the habitats of their source plants (a7 cited from https://www.inaturalist.org/photos/66336449 by © yangting, b7 cited from https://www.inaturalist.org/photos/95820686 by © sergeyprokopenko, c7 cited from https://www.inaturalist.org/photos/163584035 by © Nikolay V Dorofeev).

Scale bar in LM and SEM overview 10 μm, in SEM close-up 1 μm.

171
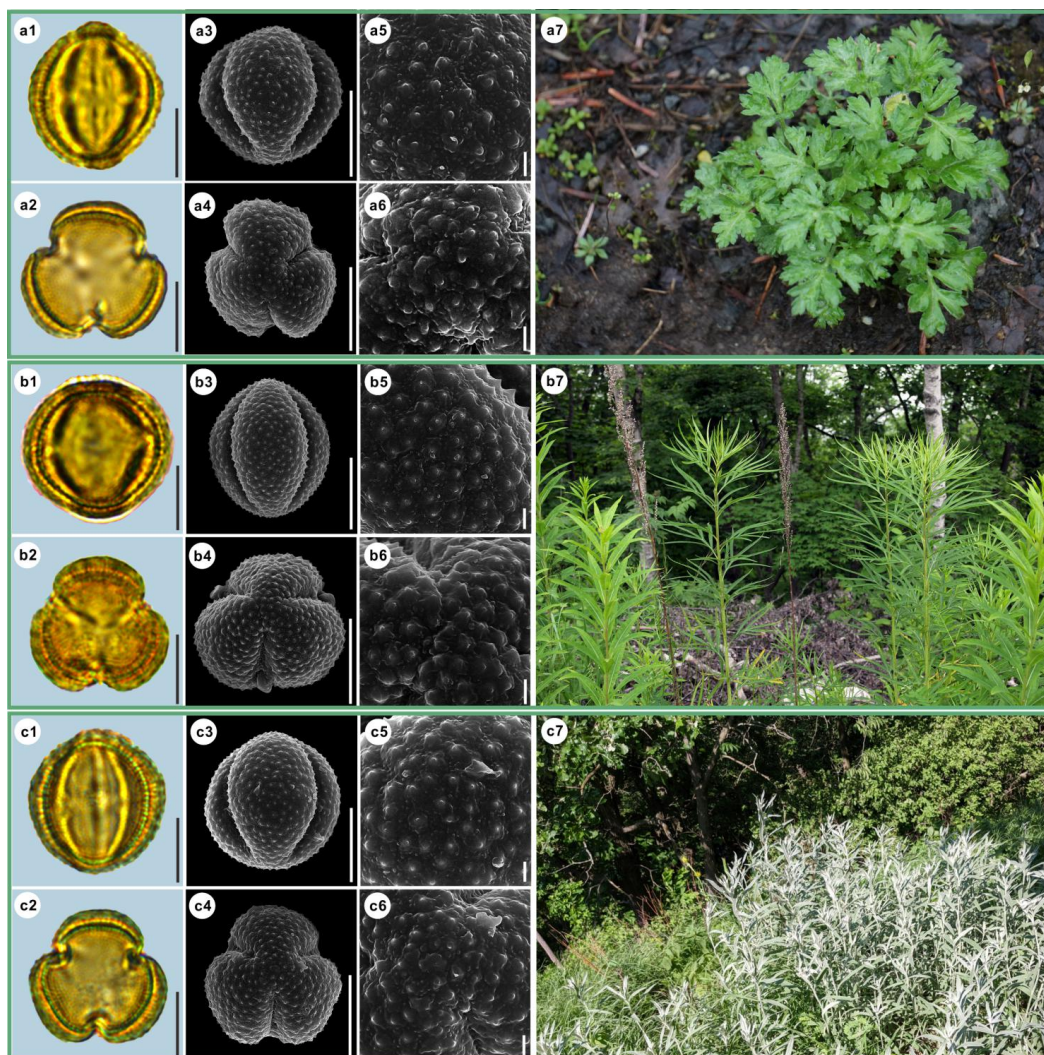
Figure 4. Pollen grains and the habitats of their source plants.

a. *Artemisia vulgaris*; b. *Artemisia selengensis*; c. *Artemisia ludoviciana*.

Pollen grains in equatorial view under LM (a1, b1, c1) and SEM (a3, a5, b3, b5, c3, c5), in polar view under LM (a2, b2, c2) and SEM (a4, a6, b4, b6, c4, c6), along with the habitats of their source plants (a7 cited from https://www.inaturalist.org/photos/120600448 by © Sara Rall, b7 cited from https://www.inaturalist.org/photos/46352423 by © Gularjanz Grigoryi Mihajlovich, c7 cited from https://www.inaturalist.org/photos/77690333 by © Ethan Rose).

Scale bar in LM and SEM overview 10 μm, in SEM close-up 1 μm.
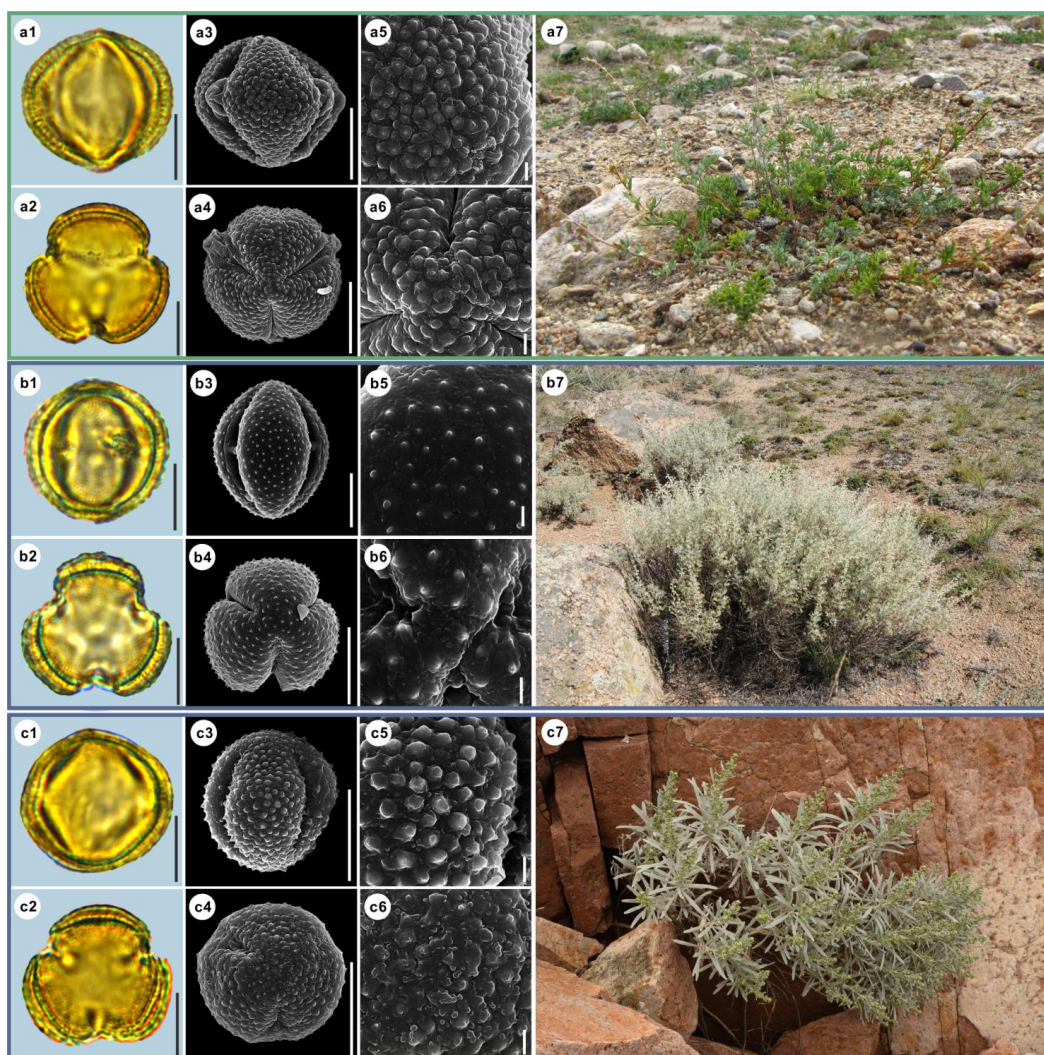
Figure 5. Pollen grains and the habitats of their source plants.

a. *Artemisia roxburghiana*; b. *Artemisia rutifolia*; c. *Artemisia chinensis*.

Pollen grains in equatorial view under LM (a1, b1, c1) and SEM (a3, a5, b3, b5, c3, c5), in polar view under LM (a2, b2, c2) and SEM (a4, a6, b4, b6, c4, c6), along with the habitats of their source plants (a7 provided by © Bo-Han Jiao, b7 cited from https://www.inaturalist.org/photos/62207191 by © Daba, c7 provided by © Jia-Hao Shen).

Scale bar in LM and SEM overview 10 μm, in SEM close-up 1 μm.

188
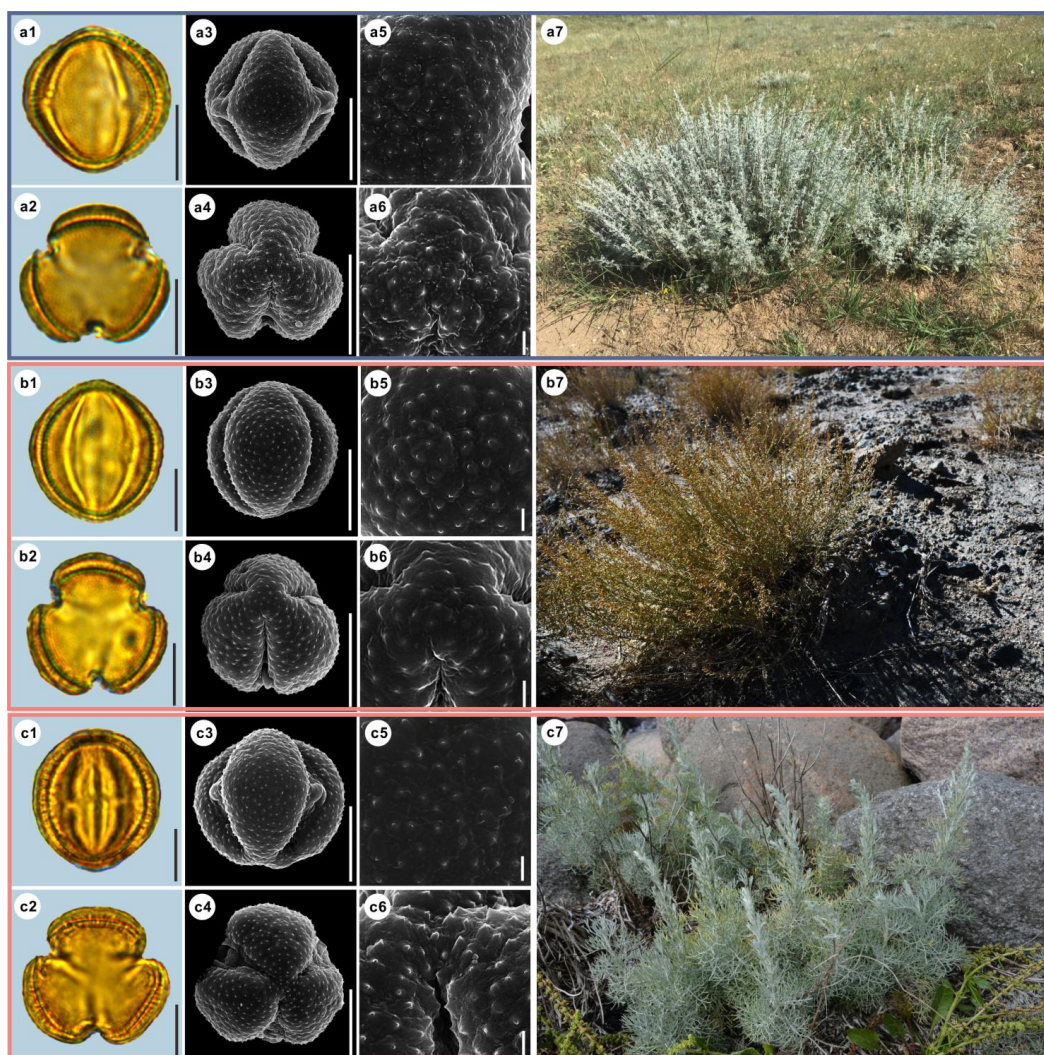
Figure 6. Pollen grains and the habitats of their source plants.

a. *Artemisia kurramensis*; b. *Artemisia compactum*; c. *Artemisia maritima*.

Pollen grains in equatorial view under LM (a1, b1, c1) and SEM (a3, a5, b3, b5, c3, c5), in polar view under
LM (a2, b2, c2) and SEM (a4, a6, b4, b6, c4, c6), along with the habitats of their source plants (a7 cited from
https://www.inaturalist.org/photos/133758174 by © Andrey Vlasenko, b7 provided by © Chen Chen, c7 cited
from https://www.inaturalist.org/photos/86515371 by © torkild).

Scale bar in LM and SEM overview 10 μm, in SEM close-up 1 μm.

196
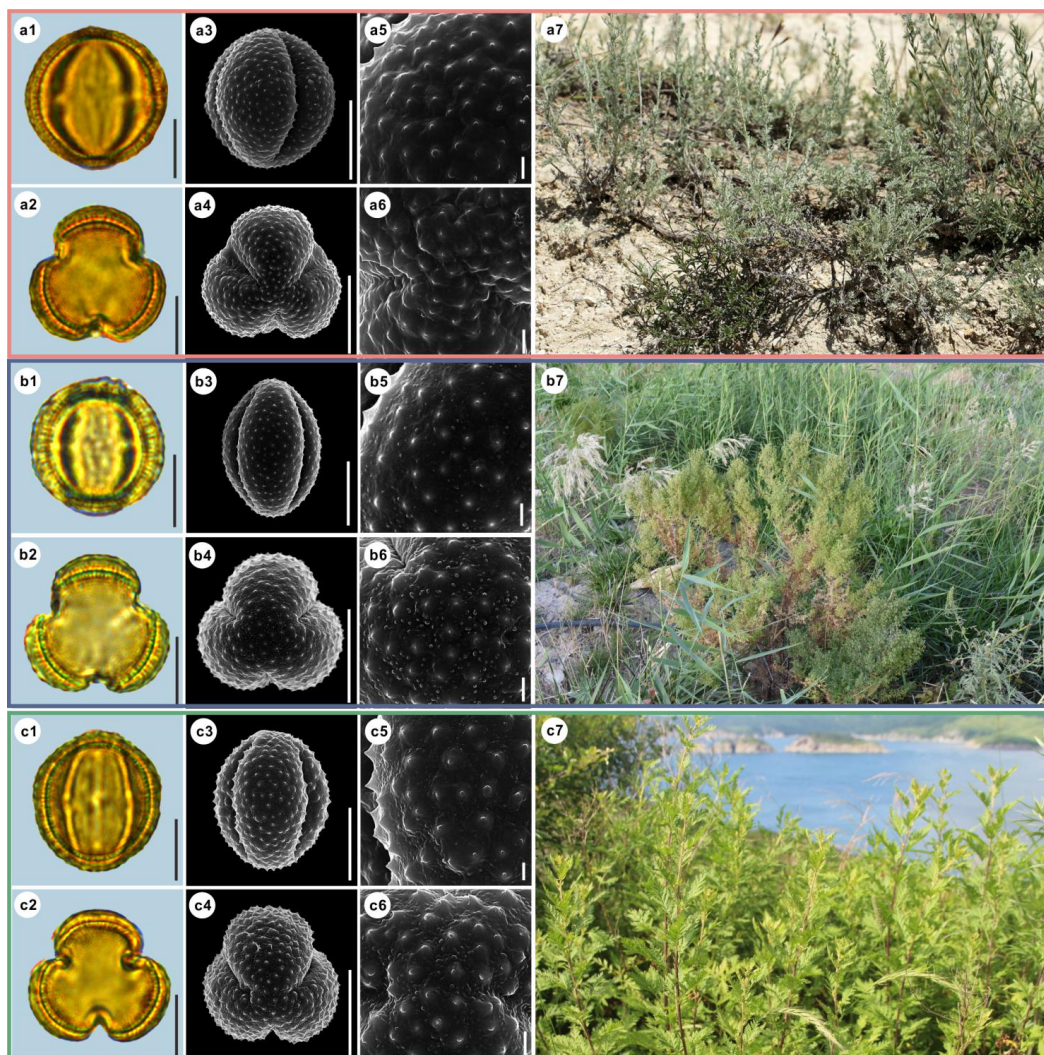
Figure 7. Pollen grains and the habitats of their source plants.

a. *Artemisia aralensis*; b. *Artemisia annua*; c. *Artemisia freyniana*.

Pollen grains in equatorial view under LM (a1, b1, c1) and SEM (a3, a5, b3, b5, c3, c5), in polar view under LM (a2, b2, c2) and SEM (a4, a6, b4, b6, c4, c6), along with the habitats of their source plants (a7 cited from https://www.inaturalist.org/photos/137114280 by © Sergey Mayorov, b7 provided by © Chen Chen, c7 cited from https://www.inaturalist.org/photos/154390279 by © Шильников Дмитрий Сергеевич).

Scale bar in LM and SEM overview 10 μm, in SEM close-up 1 μm.

204
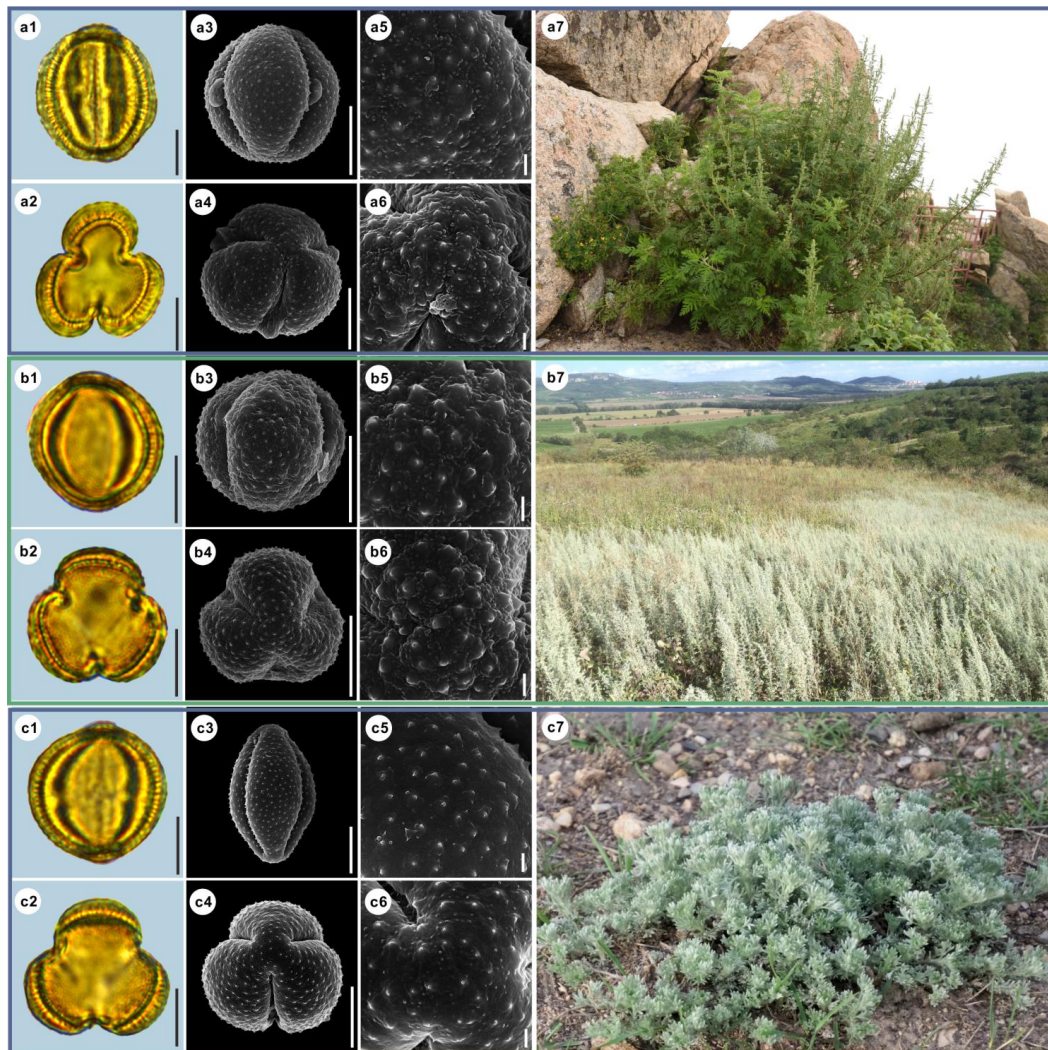
Figure 8. Pollen grains and the habitats of their source plants.

a. *Artemisia stechmanniana*; b. *Artemisia pontica*; c. *Artemisia frigida*.

Pollen grains in equatorial view under LM (a1, b1, c1) and SEM (a3, a5, b3, b5, c3, c5), in polar view under
LM (a2, b2, c2) and SEM (a4, a6, b4, b6, c4, c6), along with the habitats of their source plants (a7 provided
by © Bo-Han Jiao, b7 cited from https://www.inaturalist.org/photos/93438780 by © Martin Pražák, c7 cited
from https://www.inaturalist.org/photos/125022240 by © Suzanne Dingwell).

Scale bar in LM and SEM overview 10 μm, in SEM close-up 1 μm.

212
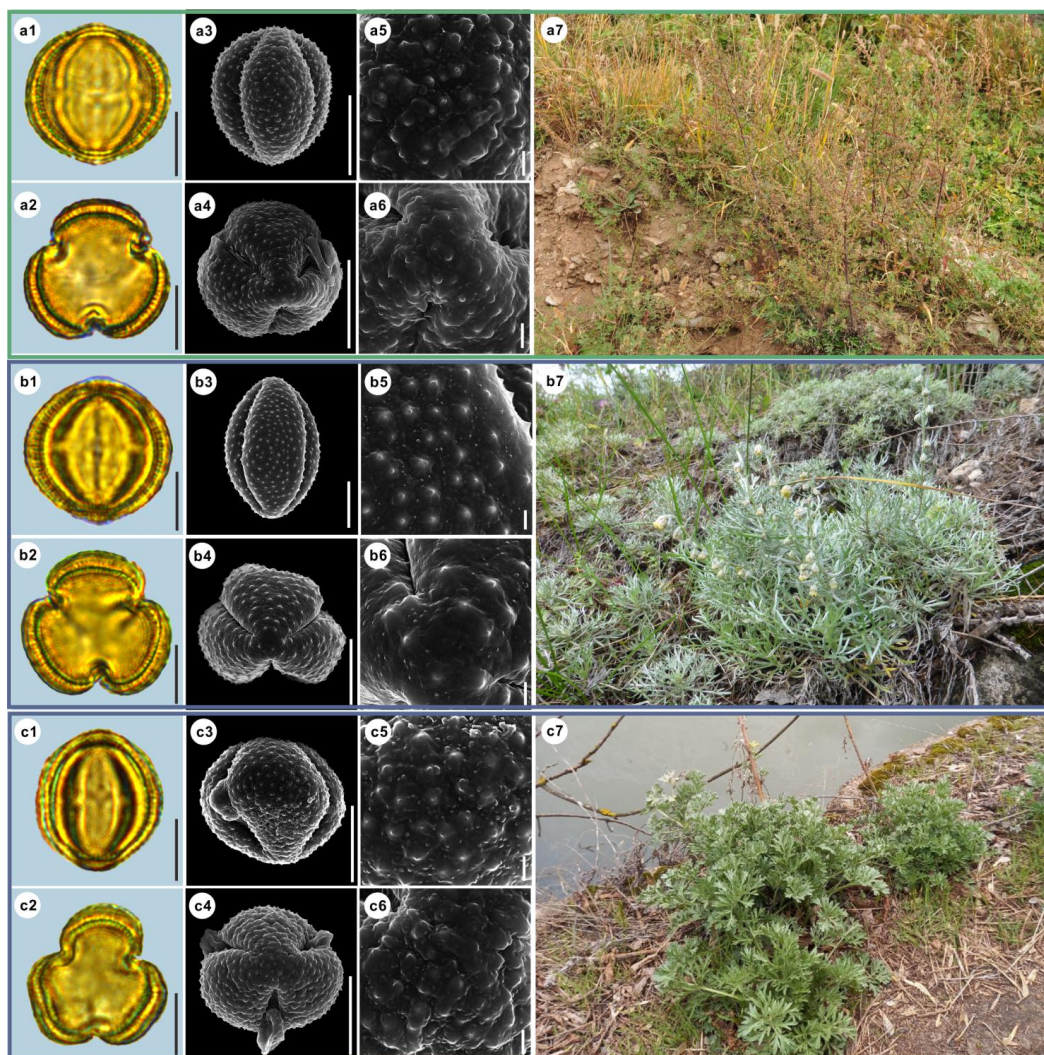
Figure 9. Pollen grains and the habitats of their source plants.

a. *Artemisia rupestris*; b. *Artemisia sericea*; c. *Artemisia absinthium*.

Pollen grains in equatorial view under LM (a1, b1, c1) and SEM (a3, a5, b3, b5, c3, c5), in polar view under LM (a2, b2, c2) and SEM (a4, a6, b4, b6, c4, c6), along with the habitats of their source plants (a7 provided by © Bo-Han Jiao, b7 cited from https://www.inaturalist.org/photos/48033353 by © svetlana_katana, c7 cited from https://www.inaturalist.org/photos/123569286 by © Станислав Лебедев).

Scale bar in LM and SEM overview 10 μm, in SEM close-up 1 μm.
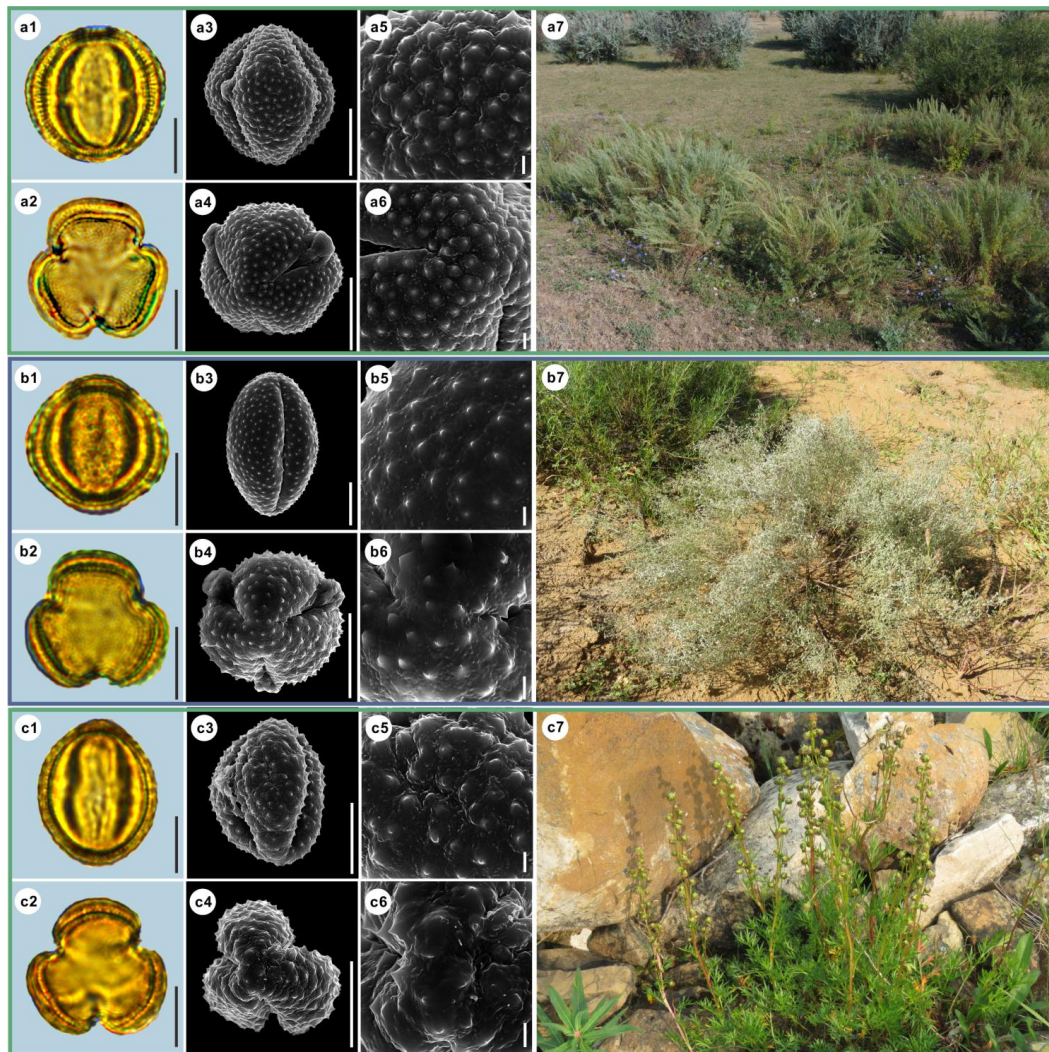
Figure 10. Pollen grains and the habitats of their source plants.

a. *Artemisia abrotanum*; b. *Artemisia blepharolepis*; c. *Artemisia norvegica*.

Pollen grains in equatorial view under LM (a1, b1, c1) and SEM (a3, a5, b3, b5, c3, c5), in polar view under LM (a2, b2, c2) and SEM (a4, a6, b4, b6, c4, c6), along with the habitats of their source plants (a7 cited from https://www.inaturalist.org/photos/116106722 by © Андрей Москвичев, b7 provided by © Ji-Ye Zheng, c7 cited from https://www.inaturalist.org/photos/161393521 by © Erin Springinotic).

Scale bar in LM and SEM overview 10 μm, in SEM close-up 1 μm.
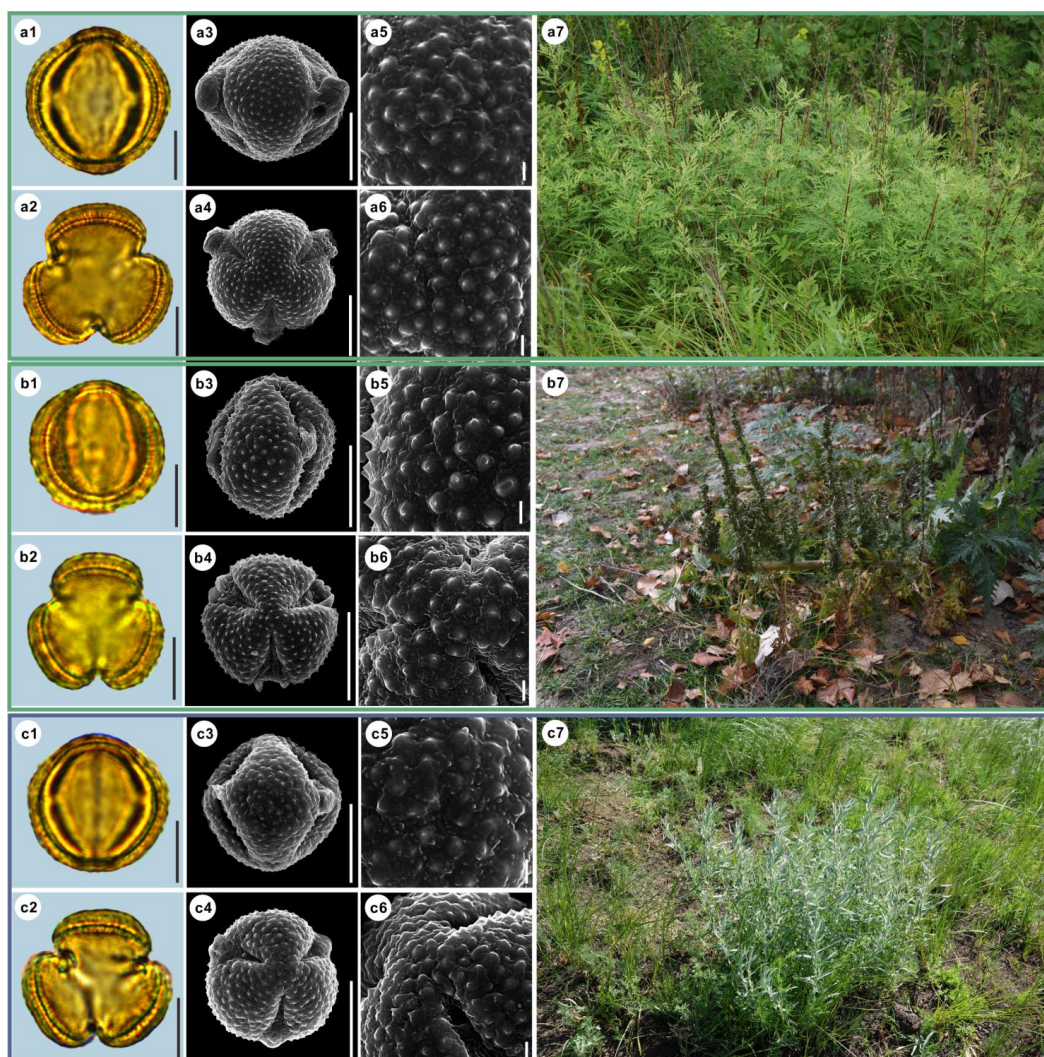
Figure 11. Pollen grains and the habitats of their source plants.

a. *Artemisia tanacetifolia*; b. *Artemisia tournefortiana*; c. *Artemisia dracunculus*.

Pollen grains in equatorial view under LM (a1, b1, c1) and SEM (a3, a5, b3, b5, c3, c5), in polar view under LM (a2, b2, c2) and SEM (a4, a6, b4, b6, c4, c6), along with the habitats of their source plants (a7 cited from https://www.inaturalist.org/photos/78902853 by © Alexander Dubynin, b7 provided by © Chen Chen, c7 cited from https://www.inaturalist.org/photos/76312868 by © anatolymikhaltsov).

Scale bar in LM and SEM overview 10 μm, in SEM close-up 1 μm.

236
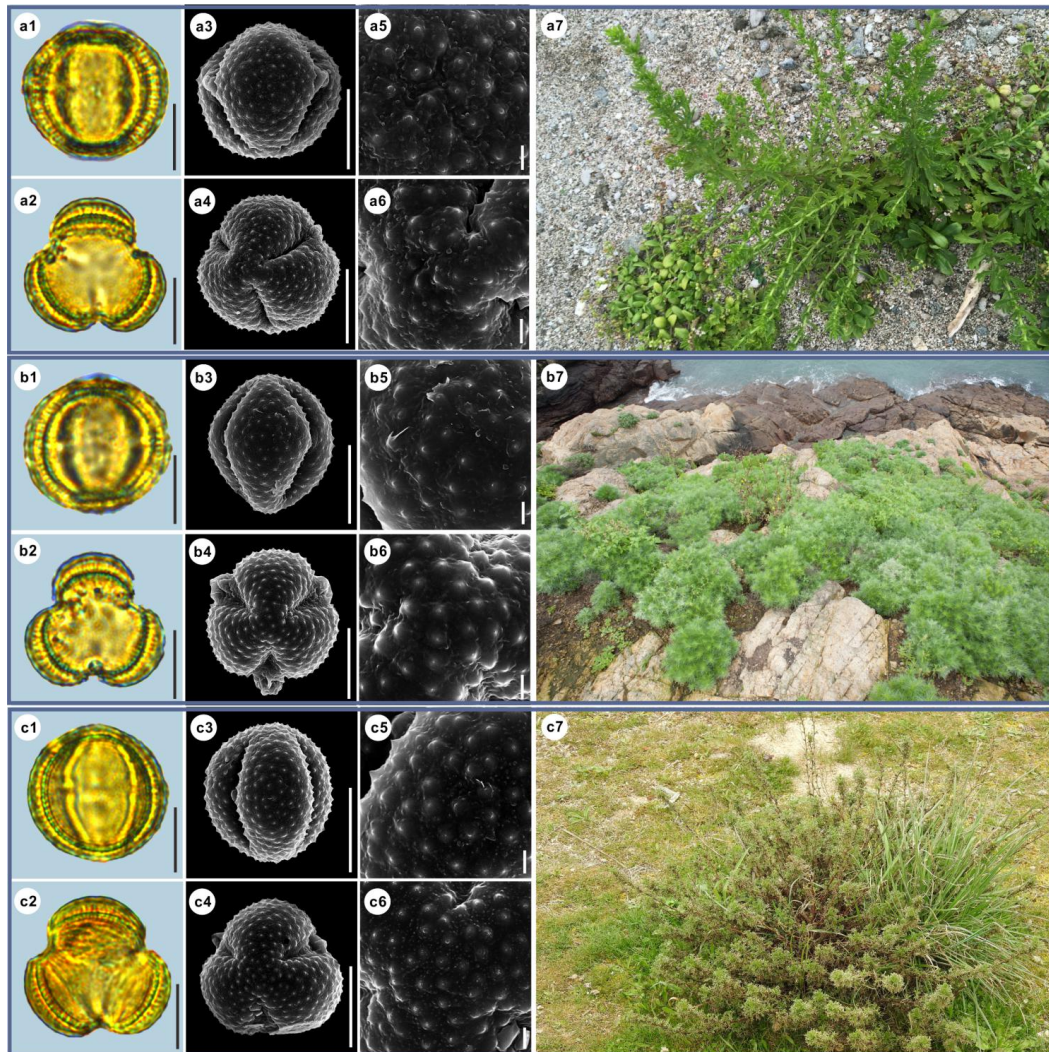
Figure 12. Pollen grains and the habitats of their source plants.

a. *Artemisia japonica*; b. *Artemisia capillaris*; c. *Artemisia campestris*.

Pollen grains in equatorial view under LM (a1, b1, c1) and SEM (a3, a5, b3, b5, c3, c5), in polar view under LM (a2, b2, c2) and SEM (a4, a6, b4, b6, c4, c6), along with the habitats of their source plants (a7 cited from https://www.inaturalist.org/photos/44507659 by © 陳達智, b7 cited from https://www.inaturalist.org/photos/60639286 by © Cheng-Tao Lin, c7 cited from https://www.inaturalist.org/photos/113822257 by © pedrosanz-anapri).

Scale bar in LM and SEM overview 10 μm, in SEM close-up 1 μm.
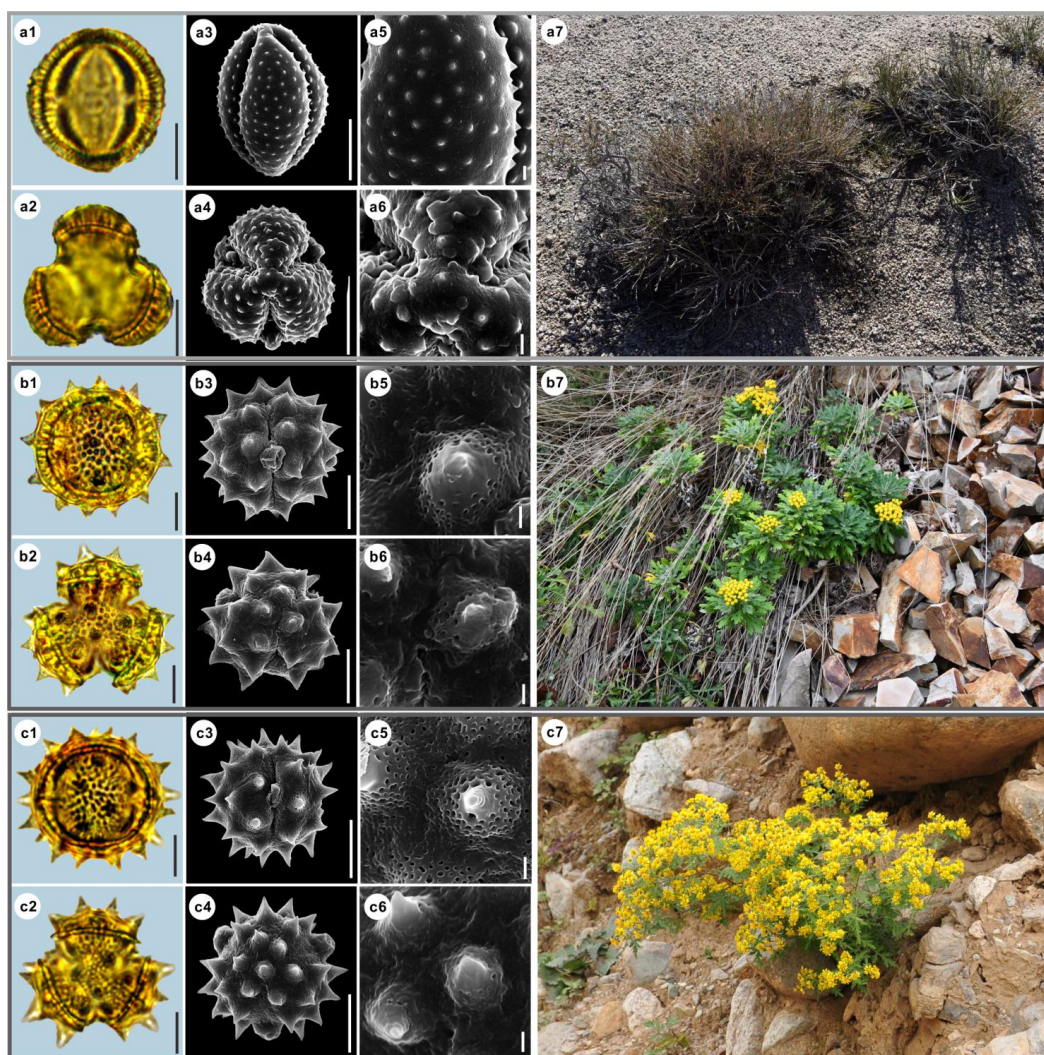
Figure 13. Pollen grains and the habitats of their source plants.

a. *Kaschgaria brachanthemoides*; b. *Ajania pallasiana*; c. *Chrysanthemum indicum*.

Pollen grains in equatorial view under LM (a1, b1, c1) and SEM (a3, a5, b3, b5, c3, c5), in polar view under LM (a2, b2, c2) and SEM (a4, a6, b4, b6, c4, c6), along with the habitats of their source plants (a7 provided by © Chen Chen, b7 cited from https://www.inaturalist.org/photos/162408714 by © Игорь Поспелов, c7 provided by © Bo-Han Jiao).

Scale bar in LM and SEM overview 10 μm, in SEM close-up 1 μm.

3.2 Statistical pollen morphological trait data of 36 sampled taxa

254 The mean values of 10 pollen morphological traits of 36 sampled species are listed in Table 1, and these data

255 distribution patterns are shown in boxplots (Fig.14) in the form of variation (25%-75%), and further described

256 in the form of mean value ± standard deviation (M ± SD, Appendix A).

257 **Table 1.** Pollen morphological traits of 36 selected species (P: Polar length; E: Equatorial width; D: Diameter
258 of spinule base; H: Spinule height; Gs: Granule spacing; Ss: Spinule spacing; Ps: Pertoration spacing).

No.	Species	P (µm)	E (µm)	P/E	D (µm)	H (µm)	D/H	Gs (µm)	Ss (µm)	Gs/Ss	Ps (µm)
1	*Artemisia cana*	23.46	24.50	0.96	0.58	0.46	1.28	0.33	1.60	0.21	0.00
2	*Artemisia tridentata*	21.36	20.69	1.04	0.76	0.60	1.30	0.24	1.12	0.22	0.00
3	*Artemisia californica*	18.94	19.13	0.99	0.75	0.71	1.08	0.24	1.45	0.17	0.00
4	*Artemisia indica*	23.47	23.81	0.99	0.76	0.39	2.04	0.28	1.21	0.24	0.00
5	*Artemisia argyi*	21.80	21.67	1.01	0.64	0.38	1.71	0.22	0.90	0.26	0.00
6	*Artemisia mongolica*	21.05	20.42	1.03	0.62	0.41	1.54	0.19	0.91	0.22	0.00
7	*Artemisia vulgaris*	19.72	19.29	1.03	0.69	0.34	2.13	0.29	1.55	0.20	0.00
8	*Artemisia selengensis*	20.67	19.68	1.06	0.67	0.38	1.76	0.22	1.05	0.22	0.00
9	*Artemisia ludoviciana*	21.65	20.82	1.04	0.70	0.37	1.94	0.20	1.23	0.16	0.00
10	*Artemisia roxburghiana*	23.88	23.69	1.01	0.76	0.39	1.96	0.28	0.79	0.36	0.00
11	*Artemisia rutifolia*	22.22	22.70	0.98	0.31	0.26	1.20	0.21	1.27	0.17	0.00
12	*Artemisia chinensis*	21.53	22.75	0.95	0.70	0.55	1.29	0.27	0.91	0.31	0.00
13	*Artemisia kurramensis*	19.71	19.35	1.02	0.38	0.27	1.41	0.23	1.25	0.19	0.00
14	*Artemisia compactum*	22.33	21.97	1.02	0.41	0.28	1.50	0.51	0.92	0.56	0.00
15	*Artemisia maritima*	26.24	23.09	1.14	0.28	0.23	1.30	0.53	1.08	0.50	0.00
16	*Artemisia aralensis*	22.32	21.91	1.02	0.25	0.22	1.16	0.50	1.09	0.46	0.00

17	*Artemisia annua*	19.71	19.45	1.02	0.45	0.39	1.18	0.27	1.29	0.21	0.00
18	*Artemisia freyniana*	23.39	21.30	1.10	0.56	0.40	1.40	0.20	1.15	0.18	0.00
19	*Artemisia stechmanniana*	26.31	25.16	1.05	0.37	0.35	1.07	0.19	1.40	0.14	0.00
20	*Artemisia pontica*	20.64	19.62	1.05	0.60	0.37	1.63	0.17	1.32	0.13	0.00
21	*Artemisia frigida*	25.11	24.90	1.01	0.46	0.32	1.44	0.31	1.30	0.24	0.00
22	*Artemisia rupestris*	24.45	22.92	1.07	0.55	0.33	1.68	0.25	0.91	0.28	0.00
23	*Artemisia sericea*	26.31	27.90	0.94	0.89	0.54	1.71	0.28	1.74	0.16	0.00
24	*Artemisia absinthium*	22.79	20.84	1.09	0.59	0.40	1.52	0.18	1.11	0.16	0.00
25	*Artemisia abrotanum*	24.47	23.73	1.03	0.72	0.51	1.44	0.22	1.41	0.16	0.00
26	*Artemisia blepharolepis*	18.96	19.26	0.99	0.69	0.44	1.64	0.37	1.68	0.23	0.00
27	*Artemisia norvegica*	24.51	22.11	1.11	0.67	0.43	1.66	0.19	1.56	0.12	0.00
28	*Artemisia tanacetifolia*	28.38	27.75	1.03	0.71	0.32	2.23	0.30	1.08	0.29	0.00
29	*Artemisia tournefortiana*	20.76	20.43	1.02	0.73	0.42	1.81	0.26	1.25	0.22	0.00
30	*Artemisia dracunculus*	22.89	22.87	1.00	0.68	0.45	1.56	0.31	0.92	0.34	0.00
31	*Artemisia japonica*	20.18	21.23	0.95	0.57	0.32	1.80	0.26	1.26	0.21	0.00
32	*Artemisia capillaris*	19.53	19.64	1.00	0.51	0.36	1.44	0.26	1.27	0.21	0.00
33	*Artemisia campestris*	21.69	21.26	1.02	0.57	0.38	1.53	0.41	1.23	0.34	0.00
34	*Kaschagaria brachanthemoides*	23.26	22.09	1.06	0.55	0.44	1.25	0.00	1.75	0.00	0.47
35	*Ajania pallasiana*	35.16	35.92	0.98	4.41	3.47	1.29	0.00	7.84	0.00	0.39
36	*Chrysanthemum indicum*	33.54	34.42	0.98	2.94	3.59	0.82	0.00	7.11	0.00	0.37
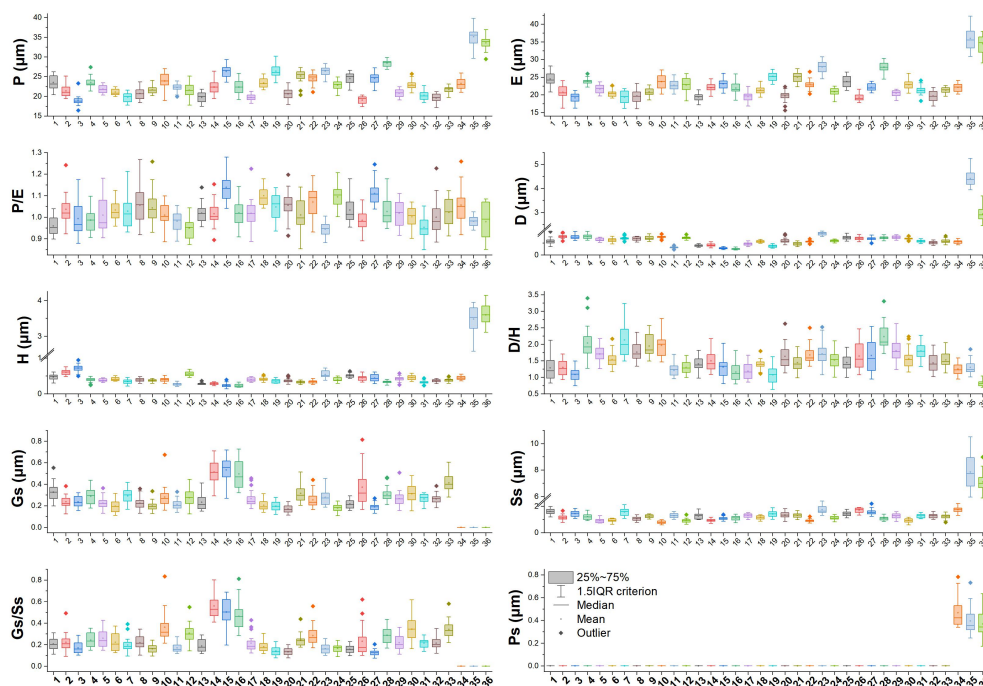
Figure 14. Boxplot of 36 sampled taxa, showing the variation in pollen morphological traits.
1. *Artemisia cana*; 2. *Artemisia tridentata*; 3. *Artemisia californica*; 4. *Artemisia indica*; 5. *Artemisia argyi*; 6. *Artemisia mongolica*; 7. *Artemisia vulgaris*; 8. *Artemisia selengensis*; 9. *Artemisia ludoviciana*; 10. *Artemisia roxburghiana*; 11. *Artemisia rutifolia*; 12. *Artemisia chinensis*; 13. *Artemisia kurramensis*; 14. *Artemisia compactum*; 15. *Artemisia maritima;* 16. *Artemisia aralensis*; 17. *Artemisia annua*; 18. *Artemisia freyniana*; 19. *Artemisia stechmanniana*; 20. *Artemisia pontica*; 21. *Artemisia frigida*; 22. *Artemisia rupestris*; 23. *Artemisia sericea*; 24. *Artemisia absinthium*; 25. *Artemisia abrotanum*; 26. *Artemisia blepharolepis*; 27. *Artemisia norvegica*; 28. *Artemisia tanacetifolia*; 29. *Artemisia tournefortiana*; 30. *Artemisia dracunculus*; 31. *Artemisia japonica*; 32. *Artemisia capillaris*; 33. *Artemisia campestris*; 34. *Kaschagaria brachanthemoides*; 35. *Ajania pallasiana*; 36. *Chrysanthemum indicum*.

3.3 The source plant occurrences

The source plant distributions in global terrestrial ecoregions of 36 sampled species are shown in Fig. 15. In *Artemisia*, some species have worldwide distributions, such as *A. vulgaris* (Fig. 15-7), *A. absinthium* (Fig. 15-24), and *A. campestris* (Fig. 15-33); a few taxa are limited to East Asia, such as *A. roxburghiana* (Fig. 15-10) and *A. blepharolepis* (Fig. 15-26), while others have narrow and isolated distributions in deserts and xeric shrublands of Central Asia, e.g. *A. kurramensis* (Fig. 15-13) and *A. aralensis* (Fig. 15-16). In outgroups of *Artemisia*, *Kaschagaria brachanthemoides* is also confined to deserts and xeric shrublands of Central Asia (Fig. 15-34), while *Ajania pallasiana* lives in forests of East Asia (Fig. 15-35).
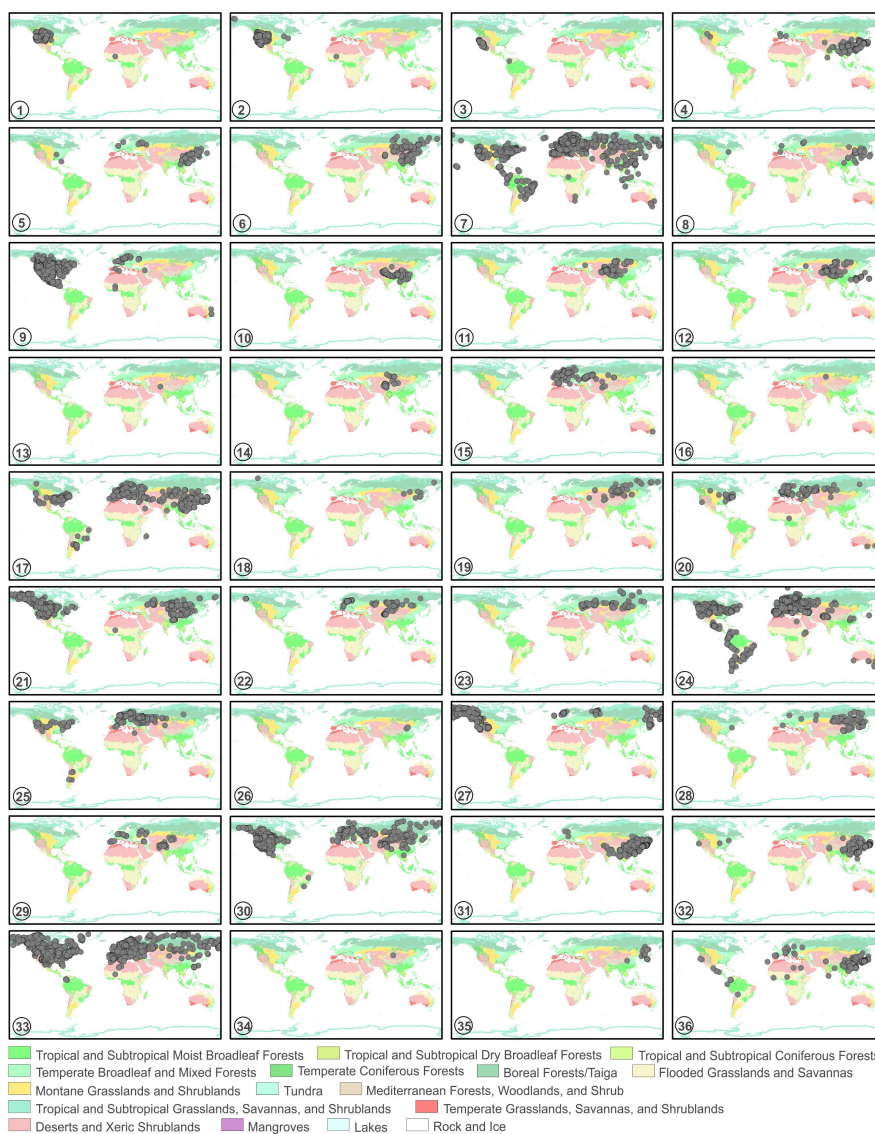
Figure 15. The global distribution maps of 36 sampled taxa in terrestrial ecoregions (modified from Olson et al., 2001).

1. *Artemisia cana*; 2. *Artemisia tridentata*; 3. *Artemisia californica*; 4. *Artemisia indica*; 5. *Artemisia argyi*; 6. *Artemisia mongolica*; 7. *Artemisia vulgaris*; 8. *Artemisia selengensis*; 9. *Artemisia ludoviciana*; 10. *Artemisia roxburghiana*; 11. *Artemisia rutifolia*; 12. *Artemisia chinensis*; 13. *Artemisia kurramensis*; 14. *Artemisia compactum*; 15. *Artemisia maritima;* 16. *Artemisia aralensis*; 17. *Artemisia annua*; 18. *Artemisia freyniana*; 19. *Artemisia stechmanniana*; 20. *Artemisia pontica*; 21. *Artemisia frigida*; 22. *Artemisia rupestris*; 23. *Artemisia sericea*; 24. *Artemisia absinthium*; 25. *Artemisia abrotanum*; 26. *Artemisia blepharolepis*; 27. *Artemisia norvegica*; 28. *Artemisia tanacetifolia*; 29. *Artemisia tournefortiana*; 30. *Artemisia dracunculus*; 31. *Artemisia japonica*; 32. *Artemisia capillaris*; 33. *Artemisia campestris*; 34. *Kaschagaria brachanthemoides*; 35. *Ajania pallasiana*; 36. *Chrysanthemum indicum*.

4 Potential use of the *Artemisia* pollen datasets

4.1 The pollen classification of *Artemisia*

The pollen grains of Anthemideae and Asteraceae under LM could be simply divided into *Artemisia* pollen type (Figs. 2-12, 13a, Appendix A) with indistinct and short spinules and *Anthemis* pollen type such as *Chrysanthemum indicum* and *Ajania pallasiana* (Figs. 13b-c, Appendix A) with distinct and long spines on pollen exine ornamentation (Wodehouse, 1926; Stix, 1960; Chen, 1987; Chen and Zhang, 1991; Martín et al., 2001; Martín et al., 2003; Sanz et al., 2008; Blackmore et al., 2009; Vallès et al., 2011). *Artemisia* pollen grains are difficult to separate from those of other related genera with *Artemisia* pollen type such as *Kaschgaria brachanthemoides* (Figs. 13a1-2, Appendix A), *Elachanthemum*, *Ajaniopsis*, *Filifolium*, and *Neopallasia* (Chen and Zhang, 1991) under LM due to their great similarity in pollen exine ornamentation and colporate patterns (Chen, 1987; Martín et al., 2001; Martín et al., 2003; Vallès et al., 2011). Furthermore, Sing and Joshi (1969) questioned the feasibility of recognizing pollen types under LM in the highly uniform pollen of *Artemisia*. Later, SEM made it possible to subdivide the pollen of *Artemisia* and those of other related genera within the *Artemisia* pollen type using pollen exine ultrastructure characters (Chen, 1987; Chen and Zhang, 1991; Sun and Xu, 1997; Jiang et al., 2005; Ghahraman et al., 2007; Shan et al., 2007; Hayat et al., 2009; Hayat et al., 2010; Hussain et al., 2019).

Hierarchical cluster analysis (Fig. 16a) revealed that the pollen morphological traits (P/E, H, D, D/H, Ss, Gs, Gs/Ss, and Ps) of *Artemisia* and its outgroups were divided into Clade A with perforations and without granules (Figs. 13a5-6, b5-6, c5-6) and Clade B with granules and without perforations (Figs. 2-12a5-6, b5-6, c5-6) on the pollen exine under SEM.
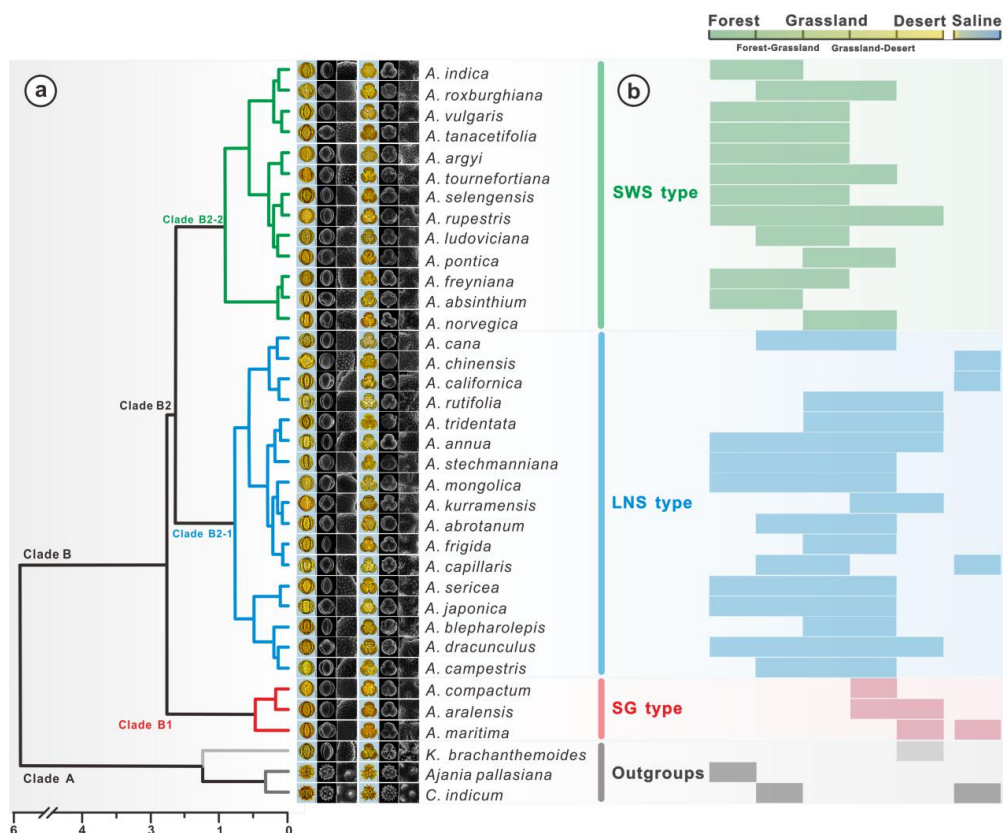
Figure 16. Hierarchical cluster analysis, showing the dendrogram for pollen types from *Artemisia* and outgroups (a) and the habitat ranges of 36 representative species (b, Tutin et al., 1976; Zhang, 2007; Ling et al., 2011).

In addition, Clade A, as the outgroup of *Artemisia*, includes both *Chrysanthemum indicum* and *Ajania pallasiana* with prominent spines on pollen exine under LM, and *Kaschgaria brachanthemoides* with spinules on pollen exine (Figs. 13a, 16a). Clade B comprises three pollen types from three branches of *Artemisia* (Fig. 16a), i.e., SG type (short and wide spinule pollen type, Clade B1), LNS type (long and narrow spinule pollen type, Clade B2-1), and SG type (sparse granule pollen type, Clade B2-2).

Nine characteristics of *Artemisia* pollen could partially explain the differences between these 3 pollen types (Fig. 17). P/E (the length of polar axis/the length of equatorial axis) in LNS types (0.93-1.06) are significantly different (ANOVA P < 0.001) from both SWS (0.97-1.12) and SG (0.98-1.14), so could be used to identify the LNS type. D/H (diameter of spinule base/spinule height) in the SWS type differ significantly (ANOVA P < 0.001) from both LNS and SG types. The variation range of D/H is 1.38-2.23 in the SWS type, 1.07-1.75 in the LNS type, and 0.98-1.66 in the SG type, indicating that the SWS pollen type is distinguished
327   by short and wide spinules. Gs/Ss (granule spacing/spinule spacing) in the SG type was higher than those of

328   the SWS and LNS types (ANOVA P < 0.001), which distinguished the SG type from the other two types.

329   Moreover, the SG type is characterized by sparse granules with the variation range of Gs/Ss spanning

330   0.37-0.64, while the SWS and LNS types show much denser granules whose Gs/Ss are mainly below 0.35.

331   Within the new *Artemisia* pollen classification (Fig. 16a, Key), the SWS type represents a type of pollen

332   with short and wide spinules (D/H > 1.81) and dense granules (Figs. 16a, 17). The LNS type is a spheroidal or

333   prolate pollen type (P/E < 0.97) with long and narrow spinules (D/H < 1.38) and dense granules (Figs. 16a,

334   17). The SG type is characterized by sparse granules (Gs/Ss > 0.37) and small, long, and narrow spinules

335   (Figs. 16a, 17).
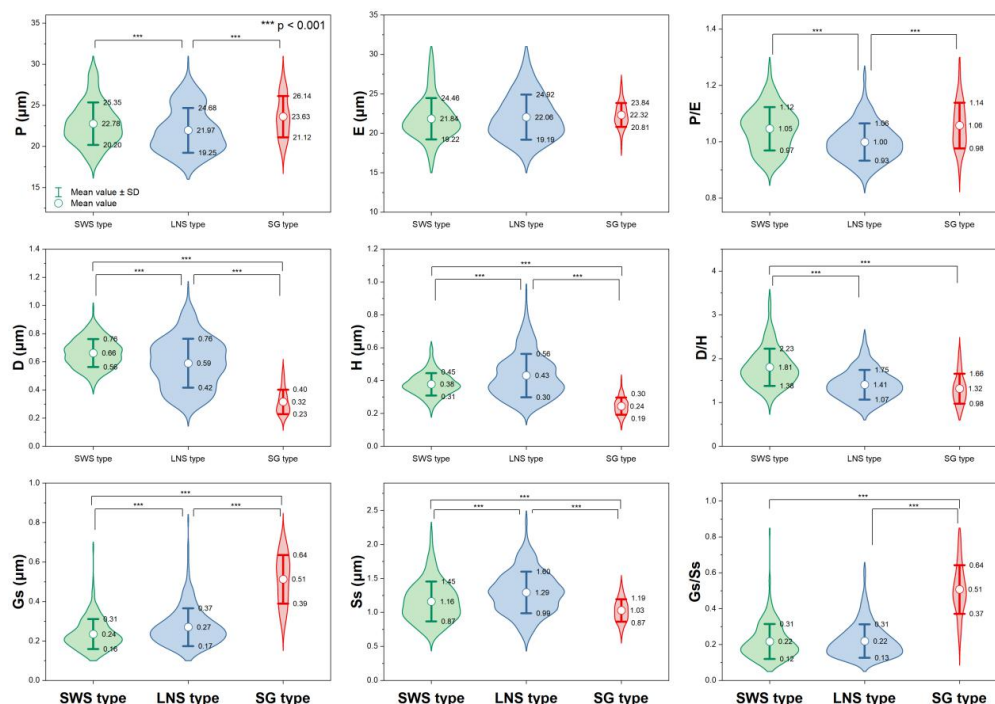
Figure 17. Violin diagram of three pollen types from *Artemisia*, showing the variations (M ± SD) in nine
pollen characters. Asterisks indicate statistically significant differences (p < 0.001).
(P: length of polar axis; E: length of equatorial axis; D: diameter of spinule base; H: spinule height; Gs:
granule spacing; Ss: spinule spacing; Ps: perforation spacing)

Key to 3 pollen types of *Artemisia* and 3 outgroups

341   1. Pollen exine with perforations and without granules under SEM ……………………………………… 2

342   1. Pollen exine with granules and without perforations under SEM ……………………………………… 3

343   2. Distinct and long spines on pollen exine, with H > 3 μm……………………*C. indicum & Ajania pallasiana*

345   2. Indistinct and short spinules on pollen exine, with H < 1μm…………………………*K. brachanthemoides*

346   3. Pollen exine with sparse granules and Gs/Ss ≥ 0.37 under SEM ………………………………… SG type

347   3. Pollen exine with dense granules and Gs/Ss ≤ 0.31 under SEM……………………………………… 4

348   4. P/E < 0.97 and pollen exine with D/H < 1.38 under SEM……………………………………… LNS type

349   4. P/E ≥ 0.97 and pollen exine with D/H ≥ 1.38 under SEM……………………………………… SWS type

4.2 The ecological implications of *Artemisia* pollen types

Plotting the distribution data of 33 species from 9 main branches of *Artemisia* constrained by the phylogenetic framework (Fig. 1) onto the global terrestrial ecoregions (Fig. 18a), we noticed that the genus is widely distributed from forest to grassland, desert, and saline habitats (Figs. 15, 16a, 18a). Furthermore, different species of *Artemisia* with SWS pollen type (Fig. 18a1) and LNS type (Fig. 18a2) have a rather wide distribution with severely overlapping ranges while those with SG type (Fig. 18a3) have narrow and isolated distributions.
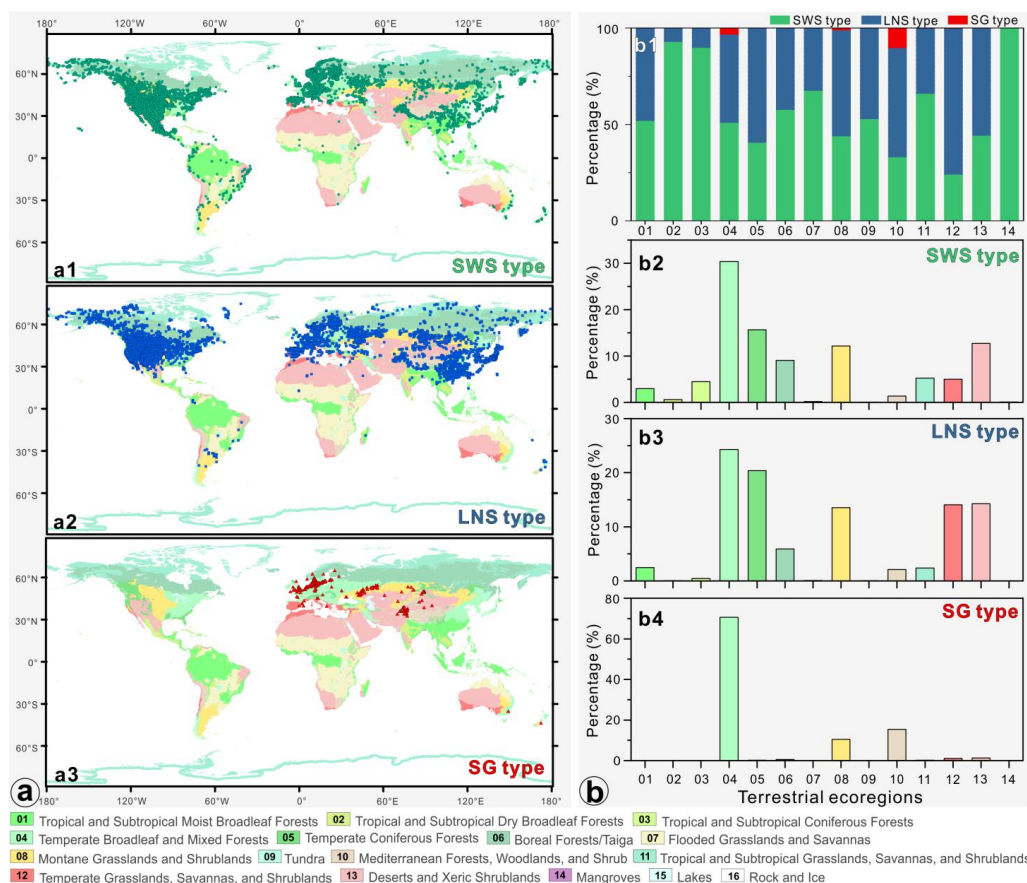
358 **Figure 18.** The global distribution pattern of 3 *Artemisia* pollen types in terrestrial ecoregions (modified from
359 Olson et al., 2001). a. The maps display the global distribution of SWS type (a1), LNS type (a2), and SG type
360 (a3). b. The histograms show the proportion of 3 pollen types in 14 terrestrial ecoregions. The proportion of
361 the three pollen types in each terrestrial ecoregion (b1) as well as the proportions of SWS type (b2), LNS type
362 (b3), and SG type (b4) in 14 ecoregions.

363   The ecological implications of *Artemisia* pollen types mentioned above fall into four categories. (i)

364 *Artemisia* with the SG pollen type all belong to the subg. *Seriphidium*, which generally grows in dry habitats

365 ranging from grassland desert to desert and coastal saline-alkaline environments (Figs. 16b, 18b1, 18b4, 19),

366 with their distribution largely limited to Eurasia and having lowest mean annual temperature (MAT) and mean

367 annual precipitation (MAP). (ii) The habitats of *Artemisia* with LNS pollen type have a global distribution and

368 occur in forest, grassland and desert, and even coastal areas (Figs. 16b, 18b1, 18b3, 19), with the highest MAT.

369 Hence, the LNS pollen type is a generalist. (iii) *Artemisia* with SWS pollen type include Sect. *Artemisia* and

370 its habitats range from forest to desert, although most of the taxa are confined to humid environments from

371 forest to grassland with a global distribution (Figs. 16b, 18b1, 18b2, 19), and the highest MAP. (iv) If the SWS

372 pollen type and the SG pollen type appear together, the range of vegetation types could be reduced to

373 grassland desert and desert through niche coexistence (Fig. 16b).
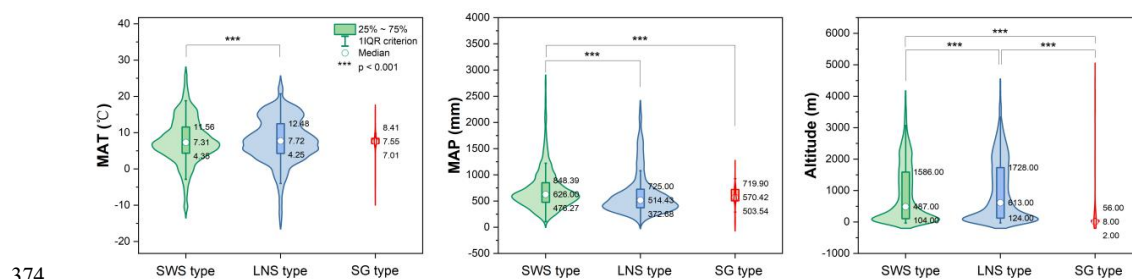
375 **Figure 19.** Violin diagram of three pollen types from *Artemisia*, showing the variations (25%-75%) in MAT,
376 MAP, and altitude. Asterisks indicate statistically significant differences (p < 0.001).

377   In addition, we noticed that *Kaschgaria brachanthemoides* as an outgroup of *Artemisia* lives in dry

378 mountain valleys or dry riverbeds of Northwest China (Toksun) and Kazakhstan, with highly characteristic

379 pollen (Fig. 12a), narrow habitats (Fig. 16b), and regional distribution (Fig. 15-34) and has the potential to

380 indicate some specific habitats.

381 **5 Data availability**

385 **Table 2.** *Artemisia* pollen datasets in this study.

Data type	Data format	Data acquisition	Data accessibility
The phylogenetic framework of *Artemisia* pollen sampling.	.png	Literature survey (modified from Malik et al., 2017).	This article
A voucher specimen list of 36 representative species.	.doc	Pollen samples were obtained from PE herbarium at the Institute of Botany, Chinese Academy of Sciences.	
12 illustrations of pollen grains and the habitats of their source plants.	.png	Habitat photos from online sources (Appendix Table A).	
4018 original pollen photographs (3205 under LM, 813 under SEM).	.jpg	Pollen samples were acetolyzed by the standard method and fixed in glycerine jelly. The pollen grains were photographed under LM and SEM using standard procedures.	Zenodo (https://doi.org /10.5281/zeno do.5842909; Lu and Jiao, 2022)
7200 statistical pollen morphological traits.	.xlsx	Statistical data of pollen morphological traits were measured by standard methods.	
30858 source plant occurrence information, and corresponding environmental factors including altitude and 19 climate parameters.	.xlsx	Their source plant distribution coordinates were obtained from GBIF (https://doi.org/10.15468/dl.596xd9). The corresponding environmental factors of these coordinates were obtained from WorldClim (https://www.worldclim.org/) with a spatial resolution of 30 seconds between 1970-2000.	

386 **6 Summary**

387 To cover the maximum range of *Artemisia* pollen morphological variation, we provide a pollen dataset of 36

388 species from 9 clades and 3 outgroups of *Artemisia* constrained by the phylogenetic framework, containing

389 high-quality pollen photographs under LM and SEM, statistical data of pollen morphological traits, together

390 with their source plant distribution, and corresponding environmental factors. Here, we attempt to decipher the

391 underlying causes of the long-standing disagreement in the palynological community on the correlation

392 between *Artemisia* pollen and aridity by recognizing the different ecological implications of *Artemisia* pollen

393 types.

394   This dataset should work well for identifying and classifying *Artemisia* pollen from Neogene sediments.

395 Based on the evidence that *Artemisia* pollen grains are consistent in morphology under LM, but different types

396 can be recognized under SEM, we could apply the single-grain technique for picking out pollen grains from

397 the Neogene sediments and photographing the same grains under LM and SEM (Ferguson et al., 2007;

398 Grímsson et al., 2011; Grímsson et al., 2012; Halbritter et al., 2018). Next, we could identify those *Artemisia*

399 pollen grains by comparison with the rich photographs from this dataset, and further recognize different

400 *Artemisia* pollen types, which provide a link to the different habitat ranges.

401   However, the application of this dataset probably may not function well for the Palaeogene, as 1)

402 *Artemisia* might have originated in the Palaeocene, but there is no evidence for a specific origin location or

403 time intervals (e.g. Ling 1982; Wang 2004; Miao 2011); 2) both the lack of macrofossils of *Artemisia* and the

404 strong pollen similarity between *Artemisia* and its closely related taxa under LM might lead to confusion and

405 more uncertainty in tracing the the origin of *Artemisia*. On the other hand, the present dataset provides a

406 potential morphological tool to distinguish *Artemisia* pollen grains from those of its related taxa at the SEM

407 level in order to solve the confusion in the Palaeogene.

408   Finally and most importantly, the *Artemisia* pollen dataset as designed is open and expandable for new

409 pollen data from *Artemisia* worldwide in order to better serve the global environment assessment and refined

410 reconstruction of vegetation in the geological past.

411 **Appendix A**

412 **Text A1**

413 Pollen morphology descriptions of 36 representative species from 9 clades of *Artemisia* and 3 outgroups.

414 **1. *Artemisia cana* (Table 1, Figs. 2a, 14)**

415 Pollen grains spheroidal or oblate. Almost circular in equatorial view and trilobate circular in polar view.
416 Apertures tricolporate. The exine near the colpi gradually thinned. Polar length (P) = 23.46 ± 1.76 μm (M ±
417 SD), equatorial width (E) = 24.50 ± 2.13 μm (M ± SD), P/E = 0.96 ± 0.04 (M ± SD). The exine ornamentation
418 is psilate (LM), spinulate (SEM). Under SEM, diameter of spinule base (D) = 0.58 ± 0.13 μm (M ± SD),
419 spinule height (H) = 0.46 ± 0.08 μm (M ± SD), D/H = 1.28 ± 0.38 (M ± SD), granule spacing (Gs) = 0.33 ±
420 0.08 μm (M ± SD), spinule spacing (Ss) = 1.60 ± 0.22 μm (M ± SD), Gs/Ss = 0.21 ± 0.06 (M ± SD).

421 Habitat: grasslands, gravel soils, mountain meadows, stream banks; Wet mountain meadows, stream banks,
422 rocky areas with late-lying snows.

423 **2. *Artemisia tridentata* (Table 1, Figs. 2b, 14)**

424 Pollen grains prolate or spheroidal. Almost circular in equatorial view and trilobate circular in polar view.
425 Apertures tricolporate. The exine near the colpi gradually thinned. P = 21.36 ± 1.54 μm, E = 20.69 ± 1.85 μm,
426 P/E = 1.04 ± 0.07. The exine ornamentation is psilate (LM), spinulate (SEM). Under SEM, D = 0.76 ± 0.08
427 μm, H = 0.60 ± 0.08 μm, D/H = 1.30 ± 0.23, Gs = 0.24 ± 0.06 μm, Ss = 1.12 ± 0.22 μm, Gs/Ss = 0.22 ± 0.08.

428 Habitat: mountains, grasslands, and meadows of western North America. Arid and semi-arid, desert, or
429 semi-desert areas of the growing shrub or semi-shrub environment.

430 **3. *Artemisia californica* (Table 1, Figs. 2c, 14)**

431 Pollen grains prolate or spheroidal or oblate. Almost circular in equatorial view and trilobate circular in polar
432 view. Apertures tricolporate. The exine near the colpi gradually thinned. P = 18.94 ± 1.30 μm, E = 19.13 ±
433 1.43 μm, P/E = 0.99 ± 0.08. The exine ornamentation is psilate (LM), spinulate (SEM). Under SEM, D = 0.75
434 ± 0.11 μm, H = 0.71 ± 0.10 μm, D/H = 1.08 ± 0.20, Gs = 0.24 ± 0.05 μm, Ss = 1.45 ± 0.23 μm, Gs/Ss = 0.17 ±
435 0.05.

436 Habitat: coastal scrub, dry foothills.

437 **4. *Artemisia indica* (Table 1, Figs. 3a, 14)**

438 Pollen grains spheroidal or oblate. Almost circular in equatorial view and trilobate circular in polar view.
439 Apertures tricolporate. The exine near the colpi gradually thinned. P = 23.47 ± 1.39 μm, E = 23.81 ± 0.86 μm,
440 P/E = 0.99 ± 0.06. The exine ornamentation is psilate (LM), spinulate (SEM). Under SEM, D = 0.76 ± 0.10
441 μm, H = 0.39 ± 0.06 μm, D/H = 2.04 ± 0.53, Gs = 0.28 ± 0.07 μm, Ss = 1.21 ± 0.24 μm, Gs/Ss = 0.24 ± 0.07.

442   Habitat: roadsides, forest margins, slopes, shrublands; low elevations to 2000 m.

443   **5. *Artemisia argyi* (Table 1, Figs. 3b, 14)**

444   Pollen grains prolate or spheroidal. Almost circular in equatorial view and trilobate circular in polar view.

445   Apertures tricolporate. The exine near the colpi gradually thinned. P = 21.80 ± 1.00 μm, E = 21.67 ± 1.27 μm,

446   P/E = 1.01 ± 0.08. The exine ornamentation is psilate (LM), spinulate (SEM). Under SEM, D = 0.64 ± 0.07

447   μm, H = 0.38 ± 0.04 μm, D/H = 1.71 ± 0.23, Gs = 0.22 ± 0.06 μm, Ss = 0.90 ± 0.17 μm, Gs/Ss = 0.26 ± 0.09.

448   Habitat: waste places, roadsides, slopes, hills, steppes, forest steppes; low elevations to 1500 m.

449   **6. *Artemisia mongolica* (Table 1, Figs. 3c, 14)**

450   Pollen grains prolate or spheroidal. Almost circular in equatorial view and trilobate circular in polar view.

451   Apertures tricolporate. The exine near the colpi gradually thinned. P = 21.05 ± 0.82 μm, E = 20.42 ± 1.01 μm,

452   P/E = 1.03 ± 0.05. The exine ornamentation is psilate (LM), spinulate (SEM). Under SEM, D = 0.62 ± 0.08

453   μm, H = 0.41 ± 0.05 μm, D/H = 1.54 ± 0.25, Gs = 0.19 ± 0.06 μm, Ss = 0.91 ± 0.14 μm, Gs/Ss = 0.22 ± 0.08.

454   Habitat: slopes, shrublands, riverbanks, lakeshores, roadsides, steppes, forest steppes, dry valleys; low

455   elevations to 2000 m.

456   **7. *Artemisia vulgaris* (Table 1, Figs. 4a, 14)**

457   Pollen grains prolate or spheroidal. Almost circular in equatorial view and trilobate circular in polar view.

458   Apertures tricolporate. The exine near the colpi gradually thinned. P = 19.72 ± 1.25 μm, E = 19.29 ± 1.82 μm,

459   P/E = 1.03 ± 0.08. The exine ornamentation is psilate (LM), spinulate (SEM). Under SEM, D = 0.69 ± 0.07

460   μm, H = 0.34 ± 0.07 μm, D/H = 2.13 ± 0.52, Gs = 0.29 ± 0.07 μm, Ss = 1.55 ± 0.32 μm, Gs/Ss = 0.20 ± 0.07.

461   Habitat: roadsides, slopes, canyons, forest margins, forest steppes, subalpine steppes; 1500-3800 m.

462   **8. *Artemisia selengensis* (Table 1, Figs. 4b, 14)**

463   Pollen grains prolate or spheroidal. Almost circular in equatorial view and trilobate circular in polar view.

464   Apertures tricolporate. The exine near the colpi gradually thinned. P = 20.67 ± 1.57 μm, E = 19.68 ± 1.94 μm,

465   P/E = 1.06 ± 0.09. The exine ornamentation is psilate (LM), spinulate (SEM). Under SEM, D = 0.67 ± 0.08

466   μm, H = 0.38 ± 0.05 μm, D/H = 1.76 ± 0.27, Gs = 0.22 ± 0.06 μm, Ss = 1.05 ± 0.15 μm, Gs/Ss = 0.22 ± 0.07.

467   Habitat: riverbanks, lakeshores, humid areas, meadows, slopes, roadsides.

468   **9. *Artemisia ludoviciana* (Table 1, Figs. 4c, 14)**

469   Pollen grains prolate or spheroidal. Almost circular in equatorial view and trilobate circular in polar view.

470   Apertures tricolporate. The exine near the colpi gradually thinned. P = 21.65 ± 1.02 μm, E = 20.82 ± 1.10 μm,

471   P/E = 1.04 ± 0.08. The exine ornamentation is psilate (LM), spinulate (SEM). Under SEM, D = 0.70 ± 0.08

472   μm, H = 0.37 ± 0.04 μm, D/H = 1.94 ± 0.31, Gs = 0.20 ± 0.05 μm, Ss = 1.23 ± 0.13 μm, Gs/Ss = 0.16 ± 0.04.

473   Habitat: disturbed roadsides, open meadows, rocky slopes.

474   **10. *Artemisia roxburghiana* (Table 1, Figs. 5a, 14)**

475   Pollen grains prolate or spheroidal. Almost circular in equatorial view and trilobate circular in polar view.

476   Apertures tricolporate. The exine near the colpi gradually thinned. P = 23.88 ± 2.04 μm, E = 23.69 ± 2.00 μm,

477   P/E = 1.01 ± 0.06. The exine ornamentation is psilate (LM), spinulate (SEM). Under SEM, D = 0.76 ± 0.07

478   μm, H = 0.39 ± 0.06 μm, D/H = 1.96 ± 0.37, Gs = 0.28 ± 0.11 μm, Ss = 0.79 ± 0.11 μm, Gs/Ss = 0.36 ± 0.14.

479   Habitat: roadsides, slopes, dry canyons, grasslands, waste areas, terraces; 700-3900 m.

480   **11. *Artemisia rutifolia* (Table 1, Figs. 5b, 14)**

481   Pollen grains spheroidal or oblate. Almost circular in equatorial view and trilobate circular in polar view.

482   Apertures tricolporate. The exine near the colpi gradually thinned. P = 22.22 ± 1.10 μm, E = 22.70 ± 1.37 μm,

483   P/E = 0.98 ± 0.05. The exine ornamentation is psilate (LM), spinulate (SEM). Under SEM, D = 0.31 ± 0.04

484   μm, H = 0.26 ± 0.04 μm, D/H = 1.20 ± 0.18, Gs = 0.21 ± 0.05 μm, Ss = 1.27 ± 0.19 μm, Gs/Ss = 0.17 ± 0.04.

485   Habitat: hills, dry river valleys, basins, steppes, semideserts, stony desert; 1300-5000 m.

486   **12. *Artemisia chinensis* (Table 1, Figs. 5c, 14)**

487   Pollen grains spheroidal or oblate. Almost circular in equatorial view and trilobate circular in polar view.

488   Apertures tricolporate. The exine near the colpi gradually thinned. P = 21.53 ± 1.95 μm, E = 22.75 ± 2.00 μm,

489   P/E = 0.95 ± 0.05. The exine ornamentation is psilate (LM), spinulate (SEM). Under SEM, D = 0.70 ± 0.05

490   μm, H = 0.55 ± 0.07 μm, D/H = 1.29 ± 0.19, Gs = 0.27 ± 0.07 μm, Ss = 0.91 ± 0.17 μm, Gs/Ss = 0.31 ± 0.09.

491   Habitat: littoral plants found on raised coral outcrops.

492   **13. *Artemisia kurramensis* (Table 1, Figs. 6a, 14)**

493   Pollen grains spheroidal. Almost circular in equatorial view and trilobate circular in polar view. Apertures

494   tricolporate. The exine near the colpi gradually thinned. P = 19.71 ± 1.28 μm, E = 19.35 ± 1.02 μm, P/E = 1.02

495   ± 0.05. The exine ornamentation is psilate (LM), spinulate (SEM). Under SEM, D = 0.38 ± 0.04 μm, H = 0.27

496   ± 0.03 μm, D/H = 1.41 ± 0.21, Gs = 0.23 ± 0.07 μm, Ss = 1.25 ± 0.21 μm, Gs/Ss = 0.19 ± 0.06.

497   Habitat: foothills, mountain slopes, dry graveyards, field borders with sparse vegetation on gravelly, fine to

498   coarse sandy-clay soils.

499   **14. *Artemisia compactum* (Table 1, Figs. 6b, 14)**

500   Pollen grains spheroidal. Almost circular in equatorial view and trilobate circular in polar view. Apertures

501   tricolporate. The exine near the colpi gradually thinned. P = 22.33 ± 1.81 μm, E = 21.97 ± 1.23 μm, P/E = 1.02

502   ± 0.06. The exine ornamentation is psilate (LM), spinulate (SEM). Under SEM, D = 0.41 ± 0.07 μm, H = 0.28

503   ± 0.03 μm, D/H = 1.50 ± 0.33, Gs = 0.51 ± 0.12 μm, Ss = 0.92 ± 0.12 μm, Gs/Ss = 0.56 ± 0.12.

504   Habitat: rocky slopes, semi-deserts, from low elevations to sub-alpine areas.

505   **15. *Artemisia maritima* (Table 1, Figs. 6c, 14)**

506   Pollen grains prolate. Almost circular in equatorial view and trilobate circular in polar view. Apertures

507   tricolporate. The exine near the colpi gradually thinned. P = 26.24 ± 1.61 μm, E = 23.09 ± 1.43 μm, P/E = 1.14

508   ± 0.06. The exine ornamentation is psilate (LM), spinulate (SEM). Under SEM, D = 0.28 ± 0.04 μm, H = 0.23

509   ± 0.06 μm, D/H = 1.30 ± 0.34, Gs = 0.53 ± 0.12 μm, Ss = 1.08 ± 0.12 μm, Gs/Ss = 0.50 ± 0.13.

510   Habitat: saltmarsh, dry and calcareous hillsides, seashores, and dry saline or alkaline soils.

511   **16. *Artemisia aralensis* (Table 1, Figs. 7a, 14)**

512   Pollen grains prolate or spheroidal. Almost circular in equatorial view and trilobate circular in polar view.

513   Apertures tricolporate. The exine near the colpi gradually thinned. P = 22.32 ± 1.72 μm, E = 21.91 ± 1.63 μm,

514   P/E = 1.02 ± 0.06. The exine ornamentation is psilate (LM), spinulate (SEM). Under SEM, D = 0.25 ± 0.04

515   μm, H = 0.22 ± 0.04 μm, D/H = 1.16 ± 0.28, Gs = 0.50 ± 0.13 μm, Ss = 1.09 ± 0.18 μm, Gs/Ss = 0.46 ± 0.14.

516   Habitat: clayey, sandy loam, solonetzic soils.

517   **17. *Artemisia annua* (Table 1, Figs. 7b, 14)**

518   Pollen grains prolate or spheroidal. Almost circular in equatorial view and trilobate circular in polar view.

519   Apertures tricolporate. The exine near the colpi gradually thinned. P = 19.71 ± 0.84 μm, E = 19.45 ± 1.32 μm,

520   P/E = 1.02 ± 0.07. The exine ornamentation is psilate (LM), spinulate (SEM). Under SEM, D = 0.45 ± 0.06

521   μm, H = 0.39 ± 0.05 μm, D/H = 1.18 ± 0.25, Gs = 0.27 ± 0.08 μm, Ss = 1.29 ± 0.16 μm, Gs/Ss = 0.21 ± 0.08.

522   Habitat: hills, waysides, wastelands, outer forest margins, steppes, forest steppes, dry flood lands, terraces,

523   semidesert steppes, rocky slopes, roadsides, saline soils; 2000-3700 m.

524   **18. *Artemisia freyniana* (Table 1, Figs. 7c, 14)**

525   Pollen grains prolate. Almost circular in equatorial view and trilobate circular in polar view. Apertures

526   tricolporate. The exine near the colpi gradually thinned. P = 23.39 ± 1.21 μm, E = 21.30 ± 1.07 μm, P/E = 1.10

527   ± 0.04. The exine ornamentation is psilate (LM), spinulate (SEM). Under SEM, D = 0.56 ± 0.05 μm, H = 0.40

528   ± 0.06 μm, D/H = 1.40 ± 0.15, Gs = 0.20 ± 0.05 μm, Ss = 1.15 ± 0.15 μm, Gs/Ss = 0.18 ± 0.05.

529   Habitat: steppes, slopes, dry river valleys, riverbanks, outer forest margins.

530   **19. *Artemisia stechmanniana* (Table 1, Figs. 8a, 14)**

531   Pollen grains prolate or spheroidal. Almost circular in equatorial view and trilobate circular in polar view.

532   Apertures tricolporate. The exine near the colpi gradually thinned. P = 26.31 ± 1.48 μm, E = 25.16 ± 1.22 μm,

533   P/E = 1.05 ± 0.07. The exine ornamentation is psilate (LM), spinulate (SEM). Under SEM, D = 0.37 ± 0.05

534   μm, H = 0.35 ± 0.05 μm, D/H = 1.07 ± 0.25, Gs = 0.19 ± 0.04 μm, Ss = 1.40 ± 0.24 μm, Gs/Ss = 0.14 ± 0.04.

535   Habitat: hillsides, roadsides, shrubland, and forest-steppe areas, and often becoming the dominant species or

536   main associated species of plant communities in some areas of mountainous sunny slopes.

537   **20. *Artemisia pontica* (Table 1, Figs. 8b, 14)**

538   Pollen grains prolate or spheroidal. Almost circular in equatorial view and trilobate circular in polar view.

539   Apertures tricolporate. The exine near the colpi gradually thinned. P = 20.64 ± 1.54 μm, E = 19.62 ± 1.59 μm,

540   P/E = 1.05 ± 0.07. The exine ornamentation is psilate (LM), spinulate (SEM). Under SEM, D = 0.60 ± 0.11

541   μm, H = 0.37 ± 0.06 μm, D/H = 1.63 ± 0.37, Gs = 0.17 ± 0.04 μm, Ss = 1.32 ± 0.27 μm, Gs/Ss = 0.13 ± 0.04.

542   Habitat: rocky slopes, dry valleys, steppes, hills; low to middle elevations.

543   **21. *Artemisia frigida* (Table 1, Figs. 8c, 14)**

544   Pollen grains prolate or spheroidal. Almost circular in equatorial view and trilobate circular in polar view.

545   Apertures tricolporate. The exine near the colpi gradually thinned. P = 25.11 ± 1.75 μm, E = 24.90 ± 1.48 μm,

546   P/E = 1.01 ± 0.07. The exine ornamentation is psilate (LM), spinulate (SEM). Under SEM, D = 0.46 ± 0.08

547   μm, H = 0.32 ± 0.04 μm, D/H = 1.44 ± 0.26, Gs = 0.31 ± 0.08 μm, Ss = 1.30 ± 0.18 μm, Gs/Ss = 0.24 ± 0.06.

548   Habitat: steppes, sub-alpine meadows, dry hillsides, stable dunes, dry waste areas; 1000-4000 m.

549   **22. *Artemisia rupestris* (Table 1, Figs. 9a, 14)**

550   Pollen grains prolate or spheroidal. Almost circular in equatorial view and trilobate circular in polar view.

551   Apertures tricolporate. The exine near the colpi gradually thinned. P = 24.45 ± 1.41 μm, E = 22.92 ± 1.40 μm,

552   P/E = 1.07 ± 0.08. The exine ornamentation is psilate (LM), spinulate (SEM). Under SEM, D = 0.55 ± 0.05

553   μm, H = 0.33 ± 0.04 μm, D/H = 1.68 ± 0.28, Gs = 0.25 ± 0.07 μm, Ss = 0.91 ± 0.11 μm, Gs/Ss = 0.28 ± 0.09.

554   Habitat: dry hills, desert or semidesert steppes, grassy marshlands, dry river valleys, riverbeds, scrub, forest

555   margins.

556   **23. *Artemisia sericea* (Table 1, Figs. 9b, 14)**

557   Pollen grains spheroidal or oblate. Almost circular in equatorial view and trilobate circular in polar view.

558   Apertures tricolporate. The exine near the colpi gradually thinned. P = 26.31 ± 1.31 μm, E = 27.90 ± 1.67 μm,

559   P/E = 0.94 ± 0.03. The exine ornamentation is psilate (LM), spinulate (SEM). Under SEM, D = 0.89 ± 0.09

560   μm, H = 0.54 ± 0.10 μm, D/H = 1.71 ± 0.36, Gs = 0.28 ± 0.07 μm, Ss = 1.74 ± 0.31 μm, Gs/Ss = 0.16 ± 0.05.

561   Habitat: Forest margins, hills, steppes, canyons, waste areas.

562   **24. *Artemisia absinthium* (Table 1, Figs. 9c, 14)**

563   Pollen grains prolate. Almost circular in equatorial view and trilobate circular in polar view. Apertures

564   tricolporate. The exine near the colpi gradually thinned. P = 22.79 ± 1.22 μm, E = 20.84 ± 1.11 μm, P/E = 1.09

565 ± 0.05. The exine ornamentation is psilate (LM), spinulate (SEM). Under SEM, D = 0.59 ± 0.05 μm, H = 0.40

566 ± 0.06 μm, D/H = 1.52 ± 0.25, Gs = 0.18 ± 0.04 μm, Ss = 1.11 ± 0.15 μm, Gs/Ss = 0.16 ± 0.04.

567 Habitat: hillsides, steppes, scrub, forest margins, often in locally moist situations; 1100-1500 m.

568 **25. *Artemisia abrotanum* (Table 1, Figs. 10a, 14)**

569 Pollen grains prolate or spheroidal. Almost circular in equatorial view and trilobate circular in polar view.

570 Apertures tricolporate. The exine near the colpi gradually thinned. P = 24.47 ± 1.56 μm, E = 23.73 ± 1.65 μm,

571 P/E = 1.03 ± 0.07. The exine ornamentation is psilate (LM), spinulate (SEM). Under SEM, D = 0.72 ± 0.10

572 μm, H = 0.51 ± 0.05 μm, D/H = 1.44 ± 0.25, Gs = 0.22 ± 0.04 μm, Ss = 1.41 ± 0.19 μm, Gs/Ss = 0.16 ± 0.04.

573 Habitat: the wasteland of western, southern, central, and southern Europe.

574 **26. *Artemisia blepharolepis* (Table 1, Figs. 10b, 14)**

575 Pollen grains spheroidal. Almost circular in equatorial view and trilobate circular in polar view. Apertures

576 tricolporate. The exine near the colpi gradually thinned. P = 18.96 ± 0.98 μm, E = 19.26 ± 0.99 μm, P/E = 0.99

577 ± 0.05. The exine ornamentation is psilate (LM), spinulate (SEM). Under SEM, D = 0.69 ± 0.09 μm, H = 0.44

578 ± 0.07 μm, D/H = 1.64 ± 0.44, Gs = 0.37 ± 0.18 μm, Ss = 1.68 ± 0.20 μm, Gs/Ss = 0.23 ± 0.14.

579 Habitat: low-altitude areas of dry slopes, grasslands, steppes, waste areas, roadsides, dunes near riverbanks.

580 **27. *Artemisia norvegica* (Table 1, Figs. 10c, 14)**

581 Pollen grains prolate. Almost circular in equatorial view and trilobate circular in polar view. Apertures

582 tricolporate. The exine near the colpi gradually thinned. P = 24.51 ± 1.40 μm, E = 22.11 ± 1.05 μm, P/E = 1.11

583 ± 0.06. The exine ornamentation is psilate (LM), spinulate (SEM). Under SEM, D = 0.67 ± 0.08 μm, H = 0.43

584 ± 0.11 μm, D/H = 1.66 ± 0.51, Gs = 0.19 ± 0.03 μm, Ss = 1.56 ± 0.24 μm, Gs/Ss = 0.12 ± 0.03.

585 Habitat: bare stony ground, Racomitrium heath, bouldery crests of solifluction terraces, and sometimes

586 hollows between rocks.

587 **28. *Artemisia tanacetifolia* (Table 1, Figs. 11a, 14)**

588 Pollen grains prolate or spheroidal. Almost circular in equatorial view and trilobate circular in polar view.

589 Apertures tricolporate. The exine near the colpi gradually thinned. P = 28.38 ± 0.90 μm, E = 27.75 ± 1.70 μm,

590 P/E = 1.03 ± 0.06. The exine ornamentation is psilate (LM), spinulate (SEM). Under SEM, D = 0.71 ± 0.06

591 μm, H = 0.32 ± 0.04 μm, D/H = 2.23 ± 0.40, Gs = 0.30 ± 0.07 μm, Ss = 1.08 ± 0.16 μm, Gs/Ss = 0.29 ± 0.07.

592 Habitat: middle and low-altitude areas of forest grasslands, grasslands, meadows, forest edges, open forests,

593 salty grasslands, grass slopes, and brushwood.

594 **29. *Artemisia tournefortiana* (Table 1, Figs. 11b, 14)**

595   Pollen grains prolate or spheroidal. Almost circular in equatorial view and trilobate circular in polar view.

596   Apertures tricolporate. The exine near the colpi gradually thinned. P = 20.76 ± 0.98 μm, E = 20.43 ± 0.83 μm,

597   P/E = 1.02 ± 0.06. The exine ornamentation is psilate (LM), spinulate (SEM). Under SEM, D = 0.73 ± 0.06

598   μm, H = 0.42 ± 0.07 μm, D/H = 1.81 ± 0.33, Gs = 0.26 ± 0.07 μm, Ss = 1.25 ± 0.20 μm, Gs/Ss = 0.22 ± 0.08.

599   Habitat: widely distributed on hills, terraces, dry flood lands, waste fields, steppes, open forests,

600   semi-marshlands.

601   **30. *Artemisia dracunculus* (Table 1, Figs. 11c, 14)**

602   Pollen grains spheroidal. Almost circular in equatorial view and trilobate circular in polar view. Apertures

603   tricolporate. The exine near the colpi gradually thinned. P = 22.89 ± 1.24 μm, E = 22.87 ± 1.32 μm, P/E = 1.00

604   ± 0.05. The exine ornamentation is psilate (LM), spinulate (SEM). Under SEM, D = 0.68 ± 0.05 μm, H = 0.45

605   ± 0.07 μm, D/H = 1.56 ± 0.31, Gs = 0.31 ± 0.10 μm, Ss = 0.92 ± 0.15 μm, Gs/Ss = 0.34 ± 0.11.

606   Habitat: dry slopes, steppes, semidesert steppes, forest steppes, forest margins, waste areas, roadsides, terraces,

607   subalpine meadows, meadow steppes, dry river valleys, rocky slopes, saline-alkaline soils; 500-3800 m.

608   **31. *Artemisia japonica* (Table 1, Figs. 12a, 14)**

609   Pollen grains spheroidal or oblate. Almost circular in equatorial view and trilobate circular in polar view.

610   Apertures tricolporate. The exine near the colpi gradually thinned. P = 20.18 ± 1.28 μm, E = 21.23 ± 1.26 μm,

611   P/E = 0.95 ± 0.05. The exine ornamentation is psilate (LM), spinulate (SEM). Under SEM, D = 0.57 ± 0.05

612   μm, H = 0.32 ± 0.05 μm, D/H = 1.80 ± 0.24, Gs = 0.26 ± 0.05 μm, Ss = 1.26 ± 0.16 μm, Gs/Ss = 0.21 ± 0.04.

613   Habitat: forest margins, waste areas, shrublands, hills, slopes, roadsides. Low elevations to 3300 m.

614   **32. *Artemisia capillaris* (Table 1, Figs. 12b, 14)**

615   Pollen grains spheroidal or oblate. Almost circular in equatorial view and trilobate circular in polar view.

616   Apertures tricolporate. The exine near the colpi gradually thinned. P = 19.53 ± 1.09 μm, E = 19.64 ± 1.62 μm,

617   P/E = 1.00 ± 0.08. The exine ornamentation is psilate (LM), spinulate (SEM). Under SEM, D = 0.51 ± 0.06

618   μm, H = 0.36 ± 0.04 μm, D/H = 1.44 ± 0.30, Gs = 0.26 ± 0.04 μm, Ss = 1.27 ± 0.16 μm, Gs/Ss = 0.21 ± 0.05.

619   Habitat: humid slopes, hills, terraces, roadsides, riverbanks; 100-2700 m.

620   **33. *Artemisia campestris* (Table 1, Figs. 12c, 14)**

621   Pollen grains prolate or spheroidal. Almost circular in equatorial view and trilobate circular in polar view.

622   Apertures tricolporate. The exine near the colpi gradually thinned. P = 21.69 ± 0.85 μm, E = 21.26 ± 0.89 μm,

623   P/E = 1.02 ± 0.07. The exine ornamentation is psilate (LM), spinulate (SEM). Under SEM, D = 0.57 ± 0.09

624   μm, H = 0.38 ± 0.05 μm, D/H = 1.53 ± 0.23, Gs = 0.41 ± 0.09 μm, Ss = 1.23 ± 0.19 μm, Gs/Ss = 0.34 ± 0.08.

625   Habitat: steppes, waste areas, rocky slopes, dune margins; 300-3100 m.

626   **34. *Kaschgaria brachanthemoides* (Table 1, Figs. 13a, 14)**

627   Pollen grains prolate or spheroidal. Almost circular in equatorial view and trilobate circular in polar view.

628   Apertures tricolporate. The exine near the colpi gradually thinned. P = 23.26 ± 1.44 μm, E = 22.09 ± 1.18 μm,

629   P/E = 1.06 ± 0.08. The exine ornamentation is psilate (LM), spinulate (SEM). Under SEM, D = 0.55 ± 0.07

630   μm, H = 0.44 ± 0.05 μm, D/H = 1.25 ± 0.20, Gs = 0 μm, Ss = 1.75 ± 0.20 μm, Gs/Ss = 0, Pertorations spacing

631   (Ps) = 0.47 ± 0.14 μm.

632   Habitat: dry mountain valleys, old dry riverbeds; 1000-1500 m.

633   **35. *Ajania pallasiana* (Table 1, Figs. 13b, 14)**

634   Pollen grains spheroidal. Almost circular in equatorial view and trilobate circular in polar view. Apertures

635   tricolporate. The exine near the colpi gradually thinned. P = 35.16 ± 2.68 μm, E = 35.92 ± 3.31 μm, P/E = 0.98

636   ± 0.03. The exine ornamentation spinose. Under SEM, D = 4.41 ± 0.35 μm, H = 3.47 ± 0.38 μm, D/H = 1.29 ±

637   0.21, Gs = 0 μm, Ss = 7.84 ± 1.25 μm, Gs/Ss = 0, Ps = 0.39 ± 0.12 μm.

638   Habitat: thickets, mountain slopes, 200-2900 m.

639   **36. *Chrysanthemum indicum* (Table 1, Figs. 13c, 14)**

640   Pollen grains prolate or spheroidal or oblate. Almost circular in equatorial view and trilobate circular in polar

641   view. Apertures tricolporate. The exine near the colpi gradually thinned. P = 33.54 ± 1.71 μm, E = 34.42 ±

642   2.46 μm, P/E = 0.98 ± 0.08. The exine ornamentation spinose. Under SEM, D = 2.94 ± 0.33 μm, H = 3.59 ±

643   0.29 μm, D/H = 0.82 ± 0.10, Gs = 0 μm, Ss = 7.11 ± 0.76 μm, Gs/Ss = 0, Ps = 0.37 ± 0.13 μm.

644   Habitat: grasslands on mountain slopes, thickets, wet places by rivers, fields, roadsides, saline places by

645   seashores, under shrubs, 100-2900 m.

646   **Appendix B**

647   **Table B1.** List of the voucher specimen in PE Herbarium, Institute of Botany, Chinese Academy of Sciences

Subgenus	Species	Specimen barcodes	Coll. No.	Habitat photograph sources
Subg. *Tridentata*	*Artemisia cana*	PE 01668975	H.Mozingo 79-97	© Jason Headley https://www.inaturalist.org/photos/54492753
	Artemisia tridentata	PE 01917565	Debreczy-Racz-Biro s.n.	© Matt Berger https://www.inaturalist.org/photos/117436654
	Artemisia californica	PE 01668942	Lewis S.Rose 69107	© Don Rideout https://www.inaturalist.org/photos/108921528
Subg. *Artemisia*, Sect. *Artemisia*	*Artemisia indica*	PE 00444597	Tian-Lun Dai 104336	© yangting https://www.inaturalist.org/photos/66336449
	Artemisia argyi	PE 00420930	K.M.Liou 9276	© sergeyprokopenko https://www.inaturalist.org/photos/95820686
	Artemisia mongolica	PE 00445665	Cheng-Yuan Yang & Zu-Gui Li 36466a	© Nikolay V Dorofeev https://www.inaturalist.org/photos/163584035
	Artemisia vulgaris	PE 01669703	P.Frost-Olsen 1833	© Sara Rall https://www.inaturalist.org/photos/120600448
	Artemisia selengensis	PE 00479106	Ming-Gang Li et al. 486	© Gularjanz Grigoryi Mihajlovich https://www.inaturalist.org/photos/46352423
	Artemisia ludoviciana	PE 01669278	W.Hess 2405	© Ethan Rose https://www.inaturalist.org/photos/77690333
	Artemisia roxburghiana	PE 00478222	Xingan collection team 70	© Bo-Han Jiao
	Artemisia rutifolia	PE 00478427	Ke Guo 12528	© Daba https://www.inaturalist.org/photos/62207191
Subg. *Pacifica*	*Artemisia chinensis*	PE 01565620	Y.Tateishi J.Murata.Y.Endo et al. 15202	© Jia-Hao Shen

Subg. *Seriphidium*	*Artemisia kurramensis*	PE 01669178	M.Togasi 1672	© Andrey Vlasenko https://www.inaturalist.org/photos/133758174
	Artemisia compactum	PE 00457459	Hexi team 313	© Chen Chen
	Artemisia maritima	No. 1338063	s.n.	© torkild https://www.inaturalist.org/photos/86515371
	Artemisia aralensis	No. 202006	s.n.	© Sergey Mayorov https://www.inaturalist.org/photos/137114280
	Artemisia annua	PE 01197344	Wen-Hong Jin-Tian, Kai-Yong Lang, Ge Yang 328	© Chen Chen
Subg. *Artemisia*, Sect. *Abrotanum* I	*Artemisia freyniana*	PE 01669030	S.Kharkevich 753	© Шильников Дмитрий Сергеевич https://www.inaturalist.org/photos/154390279
	Artemisia stechmanniana	PE 00478480	Shen-E Liu, Pei-Yun Fu et al. 4715	© Bo-Han Jiao
	Artemisia pontica	PE 01589110	Gy.Szollat & K.Dobolyi s.n.	© Martin Pražák https://www.inaturalist.org/photos/93438780
Subg. *Absinthium*	*Artemisia frigida*	PE 00444197	Ren-Chang Qin 0913	© Suzanne Dingwell https://www.inaturalist.org/photos/125022240
	Artemisia rupestris	PE 00478380	Anonymous 948	© Bo-Han Jiao
	Artemisia sericea	PE 01669585	N.Maltzev 3175	© svetlana_katana https://www.inaturalist.org/photos/48033353
	Artemisia absinthium	PE 01668816	G.Bujorean s.n.	© Станислав Лебедев https://www.inaturalist.org/photos/123569286
Subg. *Artemisia*, Sect. *Abrotanum* II	*Artemisia abrotanum*	PE 01668792	T.Leonova s.n.	© Андрей Москвичев https://www.inaturalist.org/photos/116106722
	Artemisia blepharolepis	PE 00421006	Kun-Jun Fu 7252	© Ji-Ye Zheng
Subg. *Artemisia*, Sect. *Abrotanum* III	*Artemisia norvegica*	PE 01669339	J.Haug s.n.	© Erin Springinotic https://www.inaturalist.org/photos/161393521

	Artemisia tanacetifolia	PE 00479744	T.P.Wang W.3379	© Alexander Dubynin https://www.inaturalist.org/photos/78902853
	Artemisia tournefortiana	PE 00479786	Ren-Chang Qin 2266	© Chen Chen
Subg. *Dracunculus*	*Artemisia dracunculus*	PE 00421462	Shen-E Liu et al. 8084	© anatolymikhaltsov https://www.inaturalist.org/photos/76312868
	Artemisia japonica	PE 00444874	Qianbei team 2850	© 陳達智 https://www.inaturalist.org/photos/44507659
	Artemisia capillaris	PE 00421156	Han-Chen Wang 4078	© Cheng-Tao Lin https://www.inaturalist.org/photos/60639286
	Artemisia campestris	PE 00421097	T.N.Liou L.1008	© pedrosanz-anapri https://www.inaturalist.org/photos/113822257
Outgroups	*Kaschagaria brachanthemoides*	PE 01577564	Yun-Wen Tian 22158	© Chen Chen
	Ajania pallasiana	PE 00420032	Guang-Zheng Wang 497	© Игорь Поспелов https://www.inaturalist.org/photos/162408714
	Chrysanthemum indicum	PE 01258852	Anonymous 221	© Bo-Han Jiao

648 Note: In the absence of habitat photographs of three species, habitat photographs of species with which they have close
649 phylogenetic relationships and similar habitats were used in this study instead, i.e. the habitat photograph of *Kaschagaria*
650 *komarovii* was used instead of *Kaschagaria brachanthemoides,* the habitat photograph of *Artemisia taurica* for *Artemisia*
651 *kurramensis* and *Artemisia santonicum* for *Artemisia aralensis.*

Author contributions. YFW, YFY, TGG conceived the ideas, LLL, BHJ, KQL, and BS collected the literature, LLL extracted and compiled the data, LLL, FQ, and BHJ made the statistical analysis, ML collected pictures, LLL, KQL, and BS drew the figures and tables, LLL, YFW, YFY, LJF, FQ, and GX wrote the first draft of this manuscript, DKF corrected the various versions of the manuscript, while all authors contributed substantially to revisions.

Competing interests. The authors declare that they have no conflict of interest.

Acknowledgments. We thank Dr. Jian Yang, Institute of Botany, Chinese Academy of Sciences, for his kind help in drafting graphics and Miss Chen Chen, Mr. Jia-Hao Shen and Mr. Ji-Ye Zheng, Institute of Botany, Chinese Academy of Sciences, for their enthusiastic assistance in providing habitat photographs.

Financial support. This research was supported by the Strategic Priority Research Program of the Chinese Academy of Sciences (No. XDB26000000), National Natural Science Foundation of China (Nos. 31970223, 32070240, and 42077416), and the Chinese Academy of Sciences President's International Fellowship Initiative (No. 2018VBA0016).

665 **References**

666 Beerling, D. J. and Royer, D. L.: Convergent Cenozoic CO2 history, Nat. Geosci., 4, 418-420, 2011.

667 Bhattacharya, T., Tierney, J. E., Addison, J. A., and Murray, J. W.: Ice-sheet modulation of deglacial North American
668   monsoon intensification, Nat. Geosci., 11, 848-852, https://doi.org/10.1038/s41561-018-0220-7, 2018.

669 Blackmore, S., Wortley, A. H., Skvarla, J. J., and Robinson, H., V. A. Funk, A. Susanna, Stuessy, T. F., and Bayer, R. J.
670   (Eds.): Evolution of pollen in Compositae. In Systematics, Evolution and Biogeography of the Compositae,
671   International Association of Plant Taxonomy, Vienna, 2009.

672 Bremer, K. and Humphries, C. J.: Generic monograph of the Asteraceae-Anthemideae, Bull. Nat. Hist. Mus., 23, 71-177,
673   https://www.biodiversitylibrary.org/item/19562, 1993.

674 Cai, M., Ye, P., Yang, X., and Li, C.: Vegetation and climate change in the Hetao Basin (Northern China) during the last
675   interglacial-glacial cycle, J. Asian Earth Sci., 171, 1-8, https://doi.org/10.1016/j.jseaes.2018.11.024, 2019.

676 Cao, X. Y., Tian, F., Li, K., Ni, J., Yu, X. S., Liu, L. N., and Wang, N. N.: Lake surface sediment pollen dataset for the
677   alpine meadow vegetation type from the eastern Tibetan Plateau and its potential in past climate reconstructions,
678   Earth Syst. Sci. Data, 13, 3525-3537, https://doi.org/10.5194/essd-13-3525-2021, 2021.

679 Chen, J. X., Shi, X. F., Liu, Y. G., Qiao, S. Q., Yang, S. X., Yan, S. J., Lv, H. H., Li, J. Y., Li, X. Y., and Li, C. X.:
680   Holocene vegetation dynamics in response to climate change and hydrological processes in the Bohai region, Clim.
681   Past., 16, 2509-2531, https://doi.org/10.5194/cp-16-2509-2020, 2020.

682 Chen, S. B.: Pollen Morphology of *Artemisia* L. from China: A Discussion on the Relationship between Pollen
683   Morphology of *Artemisia* L. and Allies, 1987 (in Chinese).

684 Chen, S. B. and Zhang, J. T.: A Study on Pollen Morphology of Some Chinese Genera in Tribe Anthemideae, Acta
685   Phytotaxonomica Sinica, 29, 246-251, 1991 (in Chinese).

686 China Vegetation Editorial Committee, Wu, Z. Y. (Ed.): Chinese Vegetation Science Press, Beijing, 1980 (in Chinese).

687 Cui, Q. Y., Zhao, Y., Qin, F., Liang, C., Li, Q., and Geng, R. W.: Characteristics of the modern pollen assemblages from
688   different vegetation zones in Northeast China: Implications for pollen-based climate reconstruction, Sci.
689   China-Earth Sci., 62, 1564-1577, https://doi.org/10.1007/s11430-018-9386-9, 2019.

690 Davies, C. P. and Fall, P. L.: Modern pollen precipitation from an elevational transect in central Jordan and its
691   relationship to vegetation, J. Biogeogr., 28, 1195-1210, https://doi.org/10.1046/j.1365-2699.2001.00630.x, 2001.

692 El-Moslimany, A. P.: Ecological significance of common nonarboreal pollen : examples from drylands of the Middle East,
693   Rev. Palaeobot. Palynol., 64, 343-350, https://doi.org/10.1016/0034-6667(90)90150-h, 1990.

694 Erdtman, G.: The acetolysis method, a revised descriptions, Svensk Botanisk Tidskrift, 54, 561-564, 1960.

695 Ferguson, D. K., Zetter, R., and Paudayal, K. N.: The need for the SEM in palaeopalynology, C. R. Palevol, 6, 423-430,
696   http://doi.org/10.1016/j.crpv.2007.09.018, 2007.

697 Ghahraman, A., Nourbakhsh, N., Mehdi, G. K., and Atar, F.: Pollen Morphology of *Artemisia* L. (Asteraceae) in Iran,
698   Iran. Journ. Bot., 13, 21-29, 2007.

699 GBIF. org GBIF Occurrence Download: https://doi.org/10.15468/dl.596xd9, last access: 09 November 2021.

700 Grímsson, F., Zetter, R., and Hofmann, C.: Lythrum and Peplis from the Late Cretaceous and Cenozoic of North America
701   and Eurasia: new evidence suggesting early diversification within the Lythraceae, Am. J. Bot., 98, 1801-1815,
702   https://doi.org/10.3732/ajb.1100204, 2011.

703 Grímsson, F., Zetter, R., and Leng, Q.: Diverse fossil Onagraceae pollen from a Miocene palynoflora of north-east China:
704   early steps in resolving the phytogeographic history of the family, Plant Syst. Evol., 298, 671-687,
705   https://doi.org/10.1007/s00606-011-0578-0, 2012.

706 Guiot, J. and Cramer, W.: Climate change: The 2015 Paris Agreement thresholds and Mediterranean basin ecosystems,
707   Science, 354, 465-468, https://doi.org/10.1126/science.aah5015, 2016.

708 Halbritter, H., Silvia, U., Grímsson, F., Weber, M., Zetter, R., Hesse, M., Buchner, R., Svojtka, M., and Frosch-Radivo, A.:
709   Illustrated Pollen Terminology, Springer Open, 2018.

710 Hayat, M. Q., Ashraf, M., Khan, M. A., Yasmin, G., and Jabeen, S.: Palynological study of the genus *Artemisia*
711   (Asteraceae) and its systematic implications, Pak. J. Bot., 42, 751-763, https://doi.org/10.1094/MPMI-23-4-0522,
712   2010.

713 Hayat, M. Q., Ashraf, M., Khan, M. A., Yasmin, G., Shaheen, N., and Jabeen, S.: Phylogenetic analysis of *Artemisia* L.
714   (Asteraceae) based on micromorphological traits of pollen grains, Afr. J. Biotechnol., 8, 6561-6568,
715   https://doi.org/10.1556/AMicr.56.2009.4.11, 2009.

716 Herzschuh, U., Tarasov, P., Wünnemann, B., and Kai, H.: Holocene vegetation and climate of the Alashan Plateau, NW
717   China, reconstructed from pollen data, Paleogeogr. Paleoclimatol. Paleoecol., 211, 1-17,
718   https://doi.org/10.1016/j.palaeo.2004.04.001, 2004.

719 Hesse, M., Buchner, R., Froschradivo, A., Halbritter, H., Ulrich, S., Weber, M., and Zetter, R.: Pollen Terminology : An
720   illustrated handbook, Springer, NewYork, 2009.

721 Hussain, A., Potter, D., Hayat, M. Q., Sahreen, S., and Bokhari, S. A. I.: Pollen morphology and its systematic
722   implication on some species of *Artemisia* L. from Gilgit-Baltistan Pakistan, Bangladesh J. Plant Taxon., 26, 157-168,
723   https://doi.org/10.3329/bjpt.v26i2.44576, 2019.

724 Jiang, L., Q., W., Ye, L. Z., and R., L. Y.: Pollen Morphology of *Artemisia* L. and Its Systematic Significance, Wuhan
725   Univ. J. Nat. Sci., 10, 448-454, https://doi.org/10.1007/BF02830685, 2005.

726 Koutsodendris, A., Allstadt, F. J., Kern, O. A., Kousis, I., Schwarz, F., Vannacci, M., Woutersen, A., Appel, E., Berke, M.
727   A., Fang, X. M., Friedrich, O., Hoorn, C., Salzmann, U., and Pross, J.: Late Pliocene vegetation turnover on the NE
728   Tibetan Plateau (Central Asia) triggered by early Northern Hemisphere glaciation, Glob. Planet. Change, 180,
729   117-125, https://doi.org/10.1016/j.gloplacha.2019.06.001, 2019.

730 Li, F., Sun, J., Zhao, Y., Guo, X., Zhao, W., and Zhang, K.: Ecological significance of common pollen ratios: A review,
731   Front. Earth Sci. China, 4, 253-258, https://doi.org/10.1007/s11707-010-0112-7, 2010.

732 Li, X. L., Hao, Q. Z., Wei, M. J., Andreev, A. A., Wang, J. P., Tian, Y. Y., Li, X. L., Cai, M. T., Hu, J. M., and Shi, W.:
733   Phased uplift of the northeastern Tibetan Plateau inferred from a pollen record from Yinchuan Basin, northwestern
734   China, Sci. Rep., 7, 10, https://doi.org/10.1038/s41598-017-16915-z, 2017.

735 Ling, Y. R.: On the system of the genus *Artemisia* Linn. and the relationship with allies, Bulletin of Botanical Research, 2,
736   1-60, 1982 (in Chinese).

737   Ling, Y. R., Humphries, C. J., and Gilbert, M. G.: Flora of China, The Genus *Artemisia* L., Science Press, Beijing, 2011.

738   Liu, H. Y., Wang, Y., Tian, Y. H., Zhu, J. L., and Wang, H. Y.: Climatic and anthropogenic control of surface pollen
739   assemblages   in   East   Asian   steppes,   Rev.   Palaeobot.   Palynol.,   138,   281-289,
740   https://doi.org/10.1016/j.revpalbo.2006.01.008, 2006.

741   Lu, K. Q., Qin, F., Li, Y., Xie, G., Li, J. F., Cui, Y. M., Ferguson, D. K., Yao, Y. F., Wang, G. H., and Wang, Y. F.: A new
742   approach to interpret vegetation and ecosystem changes through time by establishing a correlation between surface
743   pollen and vegetation types in the eastern central Asian desert, Paleogeogr. Paleoclimatol. Paleoecol., 551, 12,
744   https://doi.org/10.1016/j.palaeo.2020.109762, 2020.

745   Lu, L. L. and Jiao, B. H.: *Artemisia* pollen dataset for exploring the potential ecological indicators in deep time, Zenodo
746   [data set], https://doi.org/zenodo.5842909, 2022.

747   Ma, Q. F., Zhu, L. P., Wang, J. B., Ju, J. T., Lu, X. M., Wang, Y., Guo, Y., Yang, R. M., Kasper, T., Haberzettl, T., and
748   Tang, L. Y.: *Artemisia*/Chenopodiaceae ratio from surface lake sediments on the central and western Tibetan Plateau
749   and   its   application,   Paleogeogr.   Paleoclimatol.   Paleoecol.,   479,   138-145,
750   https://doi.org/10.1016/j.palaeo.2017.05.002, 2017.

751   Malik, S., Vitales, D., Hayat, M. Q., Korobkov, A. A., Garnatje, T., and Valles, J.: Phylogeny and biogeography of
752   *Artemisia* subgenus Seriphidium (Asteraceae: Anthemideae), Taxon, 66, 934-952, https://doi.org/10.12705/664.8,
753   2017.

754   Marsicek, J., Shuman, B. N., Bartlein, P. J., Shafer, S. L., and Brewer, S.: Reconciling divergent trends and millennial
755   variations in Holocene temperatures, Nature, 554, 92-96, https://doi.org/10.1038/nature25464, 2018.

756   Martín, J., Torrell, M., and Valles, J.: Palynological features as a systematic marker in *Artemisia* L. and related genera
757   (Asteraceae, Anthemideae), Plant Biol., 3, 372-378, https://doi.org/10.1055/s-2001-16462, 2001.

758   Martín, J., Torrell, M., Korobkov, A. A., and Valles, J.: Palynological features as a systematic marker in *Artemisia* L. and
759   related genera (Asteraceae, Anthemideae) - II: Implications for subtribe Artemisiinae delimitation, Plant Biol., 5,
760   85-93, https://doi.org/10.1055/s-2001-16462, 2003.

761   McClelland, H. L. O., Halevy, I., Wolf-Gladrow, D. A., Evans, D., and Bradley, A. S.: Statistical Uncertainty in
762   Paleoclimate   Proxy   Reconstructions,   Geophys.   Res.   Lett.,   48,   e2021GL092773,
763   https://doi.org/10.1029/2021GL092773, 2021.

764   Miao, Y. F., Meng, Q. Q., Fang, X. M., Yan, X. L., Wu, F. L., and Song, C. H.: Origin and development of *Artemisia*
765   (Asteraceae) in Asia and its implications for the uplift history of the Tibetan Plateau: A review, Quatern. Int., 236,
766   3-12, https://doi.org/10.1016/j.quaint.2010.08.014, 2011.

767   Moberg, A., Sonechkin, D. M., Holmgren, K., Datsenko, N. M., and Karlen, W.: Highly variable Northern Hemisphere
768   temperatures   reconstructed   from   low-   and   high-resolution   proxy   data,   Nature,   433,   613-617,
769   https://doi.org/10.1038/nature03265, 2005.

770   Mosbrugger, V., Utescher, T., and L, D. D.: Cenozoic continental climatic evolution of Central Europe, Proc. Natl. Acad.
771   Sci. U. S. A., 102, 14964-14969, https://doi.org/10.1073/pnas.0505267102, 2005.

772   Olson, D. M., Dinerstein, E., Wikramanayake, E. D., Burgess, N. D., Powell, G. V. N., Underwood, E. C., D'Amico, J. A.,
773   Itoua, I., Strand, H. E., Morrison, J. C., Loucks, C. J., Allnutt, T. F., Ricketts, T. H., Kura, Y., Lamoreux, J. F.,

774 Wettengel, W. W., Hedao, P., and Kassem, K. R.: Terrestrial ecoregions of the worlds: A new map of life on Earth,
775   Bioscience, 51, 933-938, https://doi.org/10.1641/0006-3568(2001)051[0933:teotwa]2.0.co;2, 2001.

776 Sánchez-Murillo, R., Durán-Quesada, A. M., Esquivel-Hernández, G., Rojas-Cantillano, D., and Cobb, K. M.:
777   Deciphering key processes controlling rainfall isotopic variability during extreme tropical cyclones, Nat. Commun.,
778   10, 4321, https://doi.org/10.1038/s41467-019-12062-3, 2019.

779 Sanz, M., Vilatersana, R., Hidalgo, O., Garcia-Jacas, N., Susanna, A., Schneeweiss, G. M., and Vallès, J.: Molecular
780   phylogeny and evolution of floral characters of *Artemisia* and allies (Anthemideae, Asteraceae): Evidence from
781   nrDNA ETS and ITS sequences, Taxon, 57, 66-78, https://doi.org/10.2307/25065949, 2008.

782 Shan, B. Q., He, X. L., and Chen, Y. S.: Pollen Morphology of *Artemisia* in the Loess Plateau, Acta Botanica
783   Boreali-Occidentalia Sinica, 27, 1373-1379, 2007 (in Chinese).

784 Sing, G. and Joshi, R. D.: Pollen Morphology of Some Eurasian Species of *Artemisia*, Grana Palynologica, 9, 50-62,
785   https://doi.org/10.1080/00173136909436424, 1969.

786 Stix,   E.:   Pollenmorphologische   Untersuchungen   an   Compositen,   Grana,   2,   41-104,
787   https://doi.org/10.1080/00173136009429443, 1960.

788 Sun, J. T. and Xu, Y. T.: Pollen morphology and its taxonomic significance of *Artemisia* Linn. from Shandong, Journal of
789   Shandong Normal University, 12, 186-190, 1997 (in Chinese).

790 Sun, X. J., Du, N. Q., Weng, C. Y., Lin, R. F., and Wei, K. Q.: Paleovegetation and paleoenvironment of Manasi Lake,
791   Xinjiang, N. W. China during the last 14000 years, Quaternary Sciences, 14, 239-248, 1994 (in Chinese).

792 Sun, X. J., Wang, F. Y., and Song, C. Q.: Pollen-climate response surfaces of selected taxa from northern China, Sci.
793   China Ser. D-Earth Sci., 39, 486-493, 1996.

794 Tarasov, P. E., Cheddadi, R., Guiot, J., Bottema, S., Peyron, O., Belmonte, J., Ruiz-Sanchez, V., And, F. S., and Brewer,
795   S.: A method to determine warm and cool steppe biomes from pollen data; application to the Mediterranean and
796   Kazakhstan   regions,   J.   Quat.   Sci.,   13,   335-344,
797   https://doi.org/10.1002/(SICI)1099-1417(199807/08)13:4<335::AID-JQS375>3.0, 1998.

798 Tierney, J. E., Poulsen, C. J., Montanez, I. P., Bhattacharya, T., Feng, R., Ford, H. L., Honisch, B., Inglis, G. N., Petersen,
799   S. V., Sagoo, N., Tabor, C. R., Thirumalai, K., Zhu, J., Burls, N. J., Foster, G. L., Godderis, Y., Huber, B. T., Ivany, L.
800   C., Turner, S. K., Lunt, D. J., McElwain, J. C., Mills, B. J. W., Otto-Bliesner, B. L., Ridgwell, A., and Zhang, Y. G.:
801   Past climates inform our future, Science, 370, eaay3701, https://doi.org/10.1126/science.aay3701, 2020.

802 Tutin, T. G., Persson, K., and Gutermann, W.: *Artemisia*, Flora Europaea 4, Cambridge University Press, Cambridge,
803   178-186, 1976.

804 Vallès, J., Garcia, S., Hidalgo, O., Martín, J., and Garnatje, T.: Biology, Genome Evolution, Biotechnological Issues and
805   Research Including Applied Perspectives in *Artemisia* (Asteraceae), Adv. Bot. Res., 60, 349-419, 2011.

806 Vrba, E. S.: Evolution, species and fossils-how does life evolve?, S. Afr. J. Sci., 76, 61-84, 1980.

807 Wang, F. X., Qian, N. F., Zhang, Y. L., and Yang, H. Q.: Pollen Morphology of Chinese Plants (2nd edition), Science
808   Press, Beijing, 1995 (in Chinese).

809 Wang, W. M.: On the origin and development of *Artemisia* (Asteraceae) in the geological past, Bot. J. Linnean Soc., 145,
810   331-336, https://doi.org/10.1111/j.1095-8339.2004.00287.x, 2004.

811   Wang, Y., Wang, W., Liu, L. N., Jiang, Y. J., Niu, Z. M., Ma, Y. Z., He, J., and Mensing, S. A.: Reliability of the
812   *Artemisia*/Chenopodiaceae pollen ratio in differentiating vegetation and reflecting moisture in arid and semi-arid
813   China, Holocene, 30, 858-864, https://doi.org/10.1177/0959683620902219, 2020.

814   Weng, C. Y., Sun, X. J., and Chen, Y. S.: Numerical characteristics of pollen assemblages of surface samples from the
815   West Kunlun mountains, Acta Botanica Sinica, 35, 69-79, 1993 (in Chinese).

816   Wodehouse, R. P.: Pollen Grain Morphology in the Classification of the Anthemideae, Bull. Torrey Bot. Club, 53,
817   479-485, https://doi.org/10.2307/2480028, 1926.

818   Wu, F. L., Fang, X. M., and Miao, Y. F.: Aridification history of the West Kunlun Mountains since the mid-Pleistocene
819   based on sporopollen and microcharcoal records, Paleogeogr. Paleoclimatol. Paleoecol., 547, 109680,
820   https://doi.org/10.1016/j.palaeo.2020.109680, 2020.

821   Xu, Q. H., Li, Y. C., Yang, X. L., and Zheng, Z. H.: Quantitative relationship between pollen and vegetation in northern
822   China, Sci. China Ser. D-Earth Sci., 50, 582-599, https://doi.org/10.1007/s11430-007-2044-y, 2007.

823   Yang, J., Spicer, R. A., Spicer, T. E. V., Arens, N. C., Jacques, F. M. B., Su, T., Kennedy, E. M., Herman, A. B., Steart, D.
824   C., Srivastava, G., Mehrotra, R. C., Valdes, P. J., Mehrotra, N. C., Zhou, Z. K., and Lai, J. S.: Leaf form-climate
825   relationships on the global stage: an ensemble of characters, Glob. Ecol. Biogeogr., 24, 1113-1125,
826   https://doi.org/10.1111/geb.12334, 2015.

827   Yi, S., Saito, Y., Zhao, Q. H., and Wang, P. X.: Vegetation and climate changes in the Changjiang (Yangtze River) Delta,
828   China, during the past 13,000 years inferred from pollen records, Quat. Sci. Rev., 22, 1501-1519,
829   https://doi.org/10.1016/s0277-3791(03)00080-5, 2003a.

830   Yi, S., Saito, Y., Oshima, H., Zhou, Y. Q., and Wei, H. L.: Holocene environmental history inferred from pollen
831   assemblages in the Huanghe (Yellow River) delta, China: climatic change and human impact, Quat. Sci. Rev., 22,
832   609-628, https://doi.org/10.1016/s0277-3791(02)00086-0, 2003b.

833   Zachos, J., Pagani, M., Sloan, L., Thomas, E., and Billups, K.: Trends, Rhythms, and Aberrations in Global Climate 65
834   Ma to Present, Science, 292, 686-693, https://doi.org/10.1126/science.1059412, 2001.

835   Zachos, J. C., Dickens, G. R., and Zeebe, R. E.: An early Cenozoic perspective on greenhouse warming and carbon-cycle
836   dynamics, Nature, 451, 279-283, https://doi.org/10.1038/nature06588, 2008.

837   Zhang, X. S.: Vegetation map of China and its geographic pattern: Illustration of the vegetation map of the People's
838   Republic of China (1:1 000 000), Geological Press, Beijing, 2007 (in Chinese).

839   Zhang, Y., Kong, Z. C., Wang, G. H., and Ni, J.: Anthropogenic and climatic impacts on surface pollen assemblages
840   along a precipitation gradient in north-eastern China, Glob. Ecol. Biogeogr., 19, 621-631,
841   https://doi.org/10.1111/j.1466-8238.2010.00534.x, 2010.

842   Zhao, Y., Xu, Q. H., Huang, X. Z., Guo, X. L., and Tao, S. C.: Differences of modern pollen assemblages from lake
843   sediments and surface soils in arid and semi-arid China and their significance for pollen-based quantitative climate
844   reconstruction, Rev. Palaeobot. Palynol., 156, 519-524, https://doi.org/10.1016/j.revpalbo.2009.05.001, 2009.

845   Zhao, Y., Liu, H. Y., Li, F. R., Huang, X. Z., Sun, J. H., Zhao, W. W., Herzschuh, U., and Tang, Y.: Application and
846   limitations of the *Artemisia*/Chenopodiaceae pollen ratio in arid and semi-arid China, Holocene, 22, 1385-1392,
847   https://doi.org/10.1177/0959683612449762, 2012.

848   Zhao, Y. T., Miao, Y. F., Fang, Y. M., Li, Y., Lei, Y., Chen, X. M., Dong, W. M., and An, C. B.: Investigation of factors
849   affecting surface pollen assemblages in the Balikun Basin, central Asia: Implications for palaeoenvironmental
850   reconstructions, Ecol. Indic., 123, https://doi.org/10.1016/j.ecolind.2020.107332, 2021.